TECHNICAL REPORT NUMBER 3

ANALYSIS AND OPTIMIZATION OF AN OMNI-DIRECTIONAL DIRECTION FINDING SYSTEM

Prepared by

ANTENNA RESEARCH LABORATORY

E. R. GRAF, PROJECT LEADER

December 15, 1967

CONTRACT NAS8-20557

GEORGE C. MARSHALL SPACE FLIGHT CENTER

NATIONAL AERONAUTICS AND SPACE ADMINISTRATION

HUNTSVILLE, ALABAMA

APPROVED BY:

C. H. Holmes
Head Professor
Electrical Engineering

SUBMITTED BY:

E. R. Graf
Alumni Professor of
Electrical Engineering

FOREWORD

This is a special technical report of a study conducted by the Electrical Engineering Department under the auspices of the Engineering Experiment Station toward the fulfillment of the requirements prescribed in NASA Contract NAS8-20557.

ANALYSIS AND OPTIMIZATION OF AN OMNI-DIRECTIONAL DIRECTION FINDING SYSTEM

E. R. Graf and J. M. Beste

ABSTRACT

The purpose of any direction finding system is to obtain information from which the direction of arrival of an electromagnetic wave may be determined. Conventional techniques for accomplishing this include null seeking antennas whose directional characteristics are altered mechanically or electrically, highly directional antennas which can localize a region in space, and antennas whose elements utilize time and space phase displacement. These direction finders suffer from one or more of the following disadvantages: (1) they require mechanical positioning, (2) they represent large physical structures, and (3) the direction information is redundant or is not in a readily usable form. The direction finding system described herein does not suffer from any of these disadvantages.

The direction of arrival of an electromagnetic wave above a plane earth may be uniquely described in terms of any of several space coordinate systems. In particular, the knowledge of the direction cosines with respect to two perpendicular axes, both of which lie in the horizontal plane, is necessary and sufficient to describe completely this direction of arrival. Information in the explicit form of direction cosines (or direction cosine analogs) is highly desirable in many applications. By means of simple analog circuitry, the information may be converted into that relating to other coordinate systems if this is desired.

It is well known that direction cosines appear as phase factors on the terminal voltages in linear arrays. A difficulty arises in actually determining these direction cosines by phase measurement, because of the unavoidable mutual impedances among the elements making up the array. By choosing an array with the proper spatial symmetry, and by the use of signal processing equipment, the undesirable mutual impedance effects may be eliminated from the system equations. Essentially omnidirectional antenna elements are required to observe the hemisphere above a plane earth.

In order for an operational direction finding system to derive accurate direction information, there are certain components and characteristics of the system that need to be analyzed and optimized. Both analytical and experimental work was done in this investigation, and incorporating the results into a direction finding system should produce a system capable of furnishing a phase measuring device with accurate direction information .

TABLE OF CONTENTS

LIST OF TABLES

List of Figures

I. Introduction

When a ground-based station employs scanned arrays for communicating with an orbiting space vehicle, it is obviously very important for the ground station to be able to determine the position of the space vehicle at all times.

The operational direction finding system considered in this report is designed to provide the ground station with this direction information by synthesizing two voltages with phase angles that are proportional to the direction cosines of the space vehicle. The direction cosines are referenced to two orthogonal axes at the ground station.

The direction finding system derives the direction cosines of the direction of arrival of an electromagnetic wave transmitted from a given space vehicle. Since the strength of the signal received by the direction finding antenna will be very small, it is desirable that the power dissipated in the direction finding system be minimized.

In order that the direction finding system be as efficient as possible, there must be a complete understanding of how each compoment of the system functions, and how each component should be optimized. This report is concerned with making operational an optimum direction finding system of the type previously described.

In Chapter II an analysis of how the direction information can be obtained is provided. In Chapter III an analytical study is conducted for the purpose of determining the best elements for use

in the direction finding antenna, and equations are derived for the voltages from which the direction information is obtained.

Chapter IV presents the results of an analytical study which surveyed the different components of the system in order that the components could be optimized. Chapter V contains the experimental over, in Chapter V, some of the analytical results are compared with experimental results.

II. A THEORETICAL DIRECTION FINDING SYSTEM

Consider a circular array of isotropic point sources with the coordinate system illustrated in Figure 1.

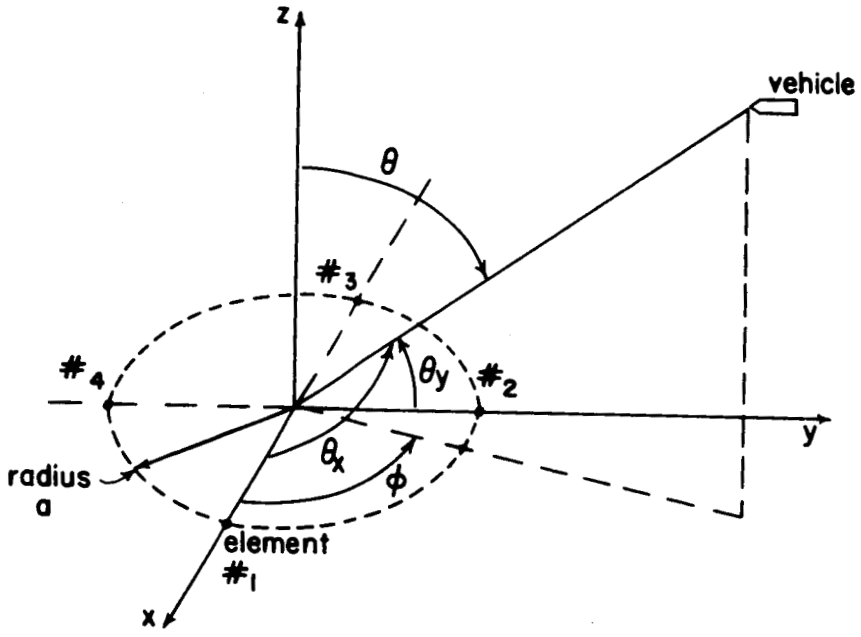

Figure 1--Coordinate System for Direction Finding Antenna.

Taking the center of the array as the phase reference, the voltages induced on the four elements by the signal transmitted from the vehicle are

$$\begin{aligned} V_1 &= V\, f_1\,(\theta,\phi)e^{\,jka\cos\Theta_x} \\ V_2 &= V\, f_2\,(\theta,\phi)e^{\,jka\cos\Theta_y} \\ V_3 &= V\, f_3\,(\theta,\phi)e^{\,-jka\cos\Theta_x} \\ V_4 &= V\, f_4\,(\theta,\phi)e^{\,-jka\cos\Theta_y} \end{aligned} \qquad (1)$$

In (1) the quantity V depends only upon the strength of the incident electromagnetic wave. The $f_i(\Theta,\Phi)$ are factors describing

the directional characteristics of the i^{th} element, and for the theoretical isotropic point sources now being considered, the $f_i(\Theta,\Phi)$ could be omitted. However, to further simplify the analysis, the $f_i(\Theta,\Phi)$ will be retained. The quantity $k = 2\pi/\lambda$, and allows dimensions to be taken in wavelengths.

The complete set of equations describing the array is:

$$
\begin{aligned}
V_1 &= I_1 Z'_{11} + I_2 Z_{12} + I_3 Z_{13} + I_4 Z_{12} \\
V_2 &= I_1 Z_{12} + I_2 Z'_{11} + I_3 Z_{12} + I_4 Z_{13} \\
V_3 &= I_1 Z_{13} + I_2 Z_{12} + I_3 Z'_{11} + I_4 Z_{12} \\
V_4 &= I_1 Z_{12} + I_2 Z_{13} + I_3 Z_{12} + I_4 Z'_{11} \quad .
\end{aligned}
\tag{2}
$$

In (2) Z'_{11} is the self-impedance, Z_{11}, of each element, plus Z, the impedance that each element sees looking into the transmission line feeding it. Z_{12} is the mutual impedance of two adjacent elements. Z_{13} is the mutual impedance between two elements diametrically across from each other.

To decouple the equations (2), four sequence voltages can be synthesized by adding the voltages from each element in four different sequences through different length transmission lines across a common load.

Thus, $V^{(o)}$ the zero sequence voltage can be obtained by adding the voltages from each element through equal length lines, obtaining

$$V^{(o)} = [\ I_1 + I_2 + I_3 + I_4\ ]\ R \quad .$$

By substituting (1) into (2) and solving for the sum of the currents, we obtain

$$V^{(0)} = \frac{VR}{Z'_{11} + 2Z_{12} + Z_{13}} \left[f_1(\Theta,\Phi)e^{jka \cos \Theta_x} + f_2(\Theta,\Phi)e^{jka \cos \Theta_y} + f_3(\Theta,\Phi)e^{-jka \cos \Theta_x} + f_4(\Theta,\Phi)e^{-jka \cos \Theta_y} \right].$$

We can form the "one" sequence by adding V_1 through a line X wavelengths, V_2 through a line X + 3/4 wavelengths, V_3 through a line X + 1/2 wavelengths, and V_4 through a line X + 1/4 wavelengths across a common load R. This operation yields

$$V^{(1)} = [I_1 + j I_2 - I_3 - j I_4] R ,$$

and, by solving (2) for the particular sum of currents, we find

$$V^{(1)} = \frac{VR}{Z'_{11} - Z_{13}} \left[f_1(\Theta,\Phi)e^{jka \cos \Theta_x} + jf_2(\Theta,\Phi)e^{jka \cos \Theta_y} - f_3(\Theta,\Phi)e^{-jka \cos\Theta_x} - jf_4(\Theta,\Phi)e^{-jka \cos \Theta_y} \right].$$

$V^{(2)}$, the second sequence voltage, can be synthesized by adding V_1 through a line X wavelengths, V_2 through a line x + 1/2 wavelengths, V_3 through a line X wavelengths, and V_4 through a line x + 1/2 wavelengths across a common load R. This operation yields:

$$V^{(2)} = [I_1 - I_2 + I_3 - I_4] R,$$

and by solving (2) for the particular sum of currents we find

$$V^{(2)} = \frac{VR}{Z_{11} - 2Z_{12} + Z_{13}} \left[f_1(\theta,\phi)e^{jka \cos \theta_x} - f_2(\theta,\phi)e^{jka \cos \theta_y} + f_3(\theta,\phi)e^{-jka \cos \theta_x} - f_4(\theta,\phi)e^{-jka \cos \theta_y} \right] .$$

$V^{(3)}$, the third sequence voltage, can be synthesized by adding V_1 through a line X wavelengths, V_2 through a line $X + 1/4$ wavelengths, V_3 through a line $X + 1/2$ wavelengths and V_4 through a line $X + 3/4$ wavelengths across a common load R. This operation yields

$$V^{(3)} = [I_1 - j I_2 - I_3 + j I_4] R ,$$

and by solving (2) for the particular sum of currents, we obtain

$$V^{(3)} = \frac{VR}{Z_{11} - Z_{13}} \left[f_1(\theta,\phi)e^{jka \cos \theta_x} - jf_2(\theta,\phi)e^{jka \cos \theta_y} - f_3(\theta,\phi)e^{-jka \cos \theta_x} + jf_4(\theta,\phi)e^{-jka \cos \theta_y} \right] .$$

The sequence voltages may now be written:

$$V^{(o)} = \frac{VR}{|Z^{(o)}|} e^{-j\phi_o} \left[f_1(\theta,\phi)e^{-jcl} + f_2(\theta,\phi)e^{-jcm} + f_3(\theta,\phi)e^{jcl} + f_4(\theta,\phi)e^{jcm} \right]$$

$$V^{(1)} = \frac{VR}{|Z^{(1)}|} e^{-j\phi_1} \left[f_1(\theta,\phi)e^{-jcl} + jf_2(\theta,\phi)e^{-jcm} - f_3(\theta,\phi)e^{jcl} - jf_4(\theta,\phi)e^{jcm} \right]$$

$$V^{(2)} = \frac{VR}{|Z^{(2)}|} e^{-j\phi 2} \left[f_1(\theta,\phi)e^{-jcl} - f_2(\theta,\phi)e^{-jcm} + f_3(\theta,\phi)e^{jcl} - f_4(\theta,\phi)e^{jcm} \right]$$

(3)

$$V^{(3)} = \frac{VR}{|Z^{(3)}|} e^{-j\phi_3} \left[f_1(\theta,\phi)e^{-jcl} - jf_2(\theta,\phi)e^{-jcm} - f_3(\theta,\phi)^{jcl} + jf_4(\theta,\phi)e^{jcm} \right],$$

where $|Z^{(i)}|$ is the magnitude of the $i^{\underline{th}}$ sequence impedance, and ϕ_i is the phase of the $i^{\underline{th}}$ sequence impedance, and

$$\begin{aligned} cl &= -ka \cos \theta_x \\ cm &= -ka \cos \theta_y \end{aligned} .$$

Before the direction cosines can be synthesized, equations (3) must be normalized, which can be achieved by adding the correct amount of attenuation and phase. After normalization, the sequence voltages may be written:

$$\begin{aligned} V^{(o)}{}_N &= f_1(\theta,\phi)e^{-jcl} + f_2(\theta,\phi)e^{-jcm} + f_3(\theta,\phi)e^{jcl} + f_4(\theta,\phi)e^{jcm} \\ V^{(1)}{}_N &= f_1(\theta,\phi)e^{-jcl} + jf_2(\theta,\phi)e^{-jcm} - f_3(\theta,\phi)e^{jcl} - jf_4(\theta,\phi)e^{jcm} \\ V^{(2)}{}_N &= f_1(\theta,\phi)e^{-jcl} - f_2(\theta,\phi)e^{-jcm} + f_3(\theta,\phi)e^{jcl} - f_4(\theta,\phi)e^{jcm} \\ V^{(3)}{}_N &= f_1(\theta,\phi)e^{-jcl} - jf_2(\theta,\phi)e^{-jcm} - f_3(\theta,\phi)e^{jcl} + jf_4(\theta,\phi)e^{jcm} . \end{aligned} \tag{4}$$

Now two voltages with phase angles directly proportional to $\cos \theta_x$ and $\cos \theta_y$ may be synthesized by properly combining equations (4):

$$V_l = V_N^{(o)} + V_N^{(1)} + V_N^{(2)} + V_N^{(3)} = 4f_1(\theta,\phi)e^{-jcl} \tag{5}$$

$$V_m = V_N^{(o)} - jV_N^{(1)} - V_N^{(2)} + jV_N^{(3)} = 4f_2(\theta,\phi)e^{-jcm} \tag{6}$$

The direction cosines now appear explicitly as the only phase factors on the voltages V_1 and V_m if the $f_i(\Theta,\Phi)$ have no phase variations with Θ or Φ. A reference voltage which contains no phase variation is necessary for phase measurements. The obvious choice (for most elements of practical importance) is:

$$V_{Ref} = V_N^{(o)} = f_1(\Theta,\Phi)e^{-jcl} + f_2(\Theta,\Phi)e^{-jcm} + f_3(\Theta,\Phi)e^{jcl} + f_4(\Theta,\Phi)e^{jcm} , \tag{7}$$

for the phase of $V_N^{(o)}$ is invariant so long as the $f_i(\Theta,\Phi)$ have no phase variation.

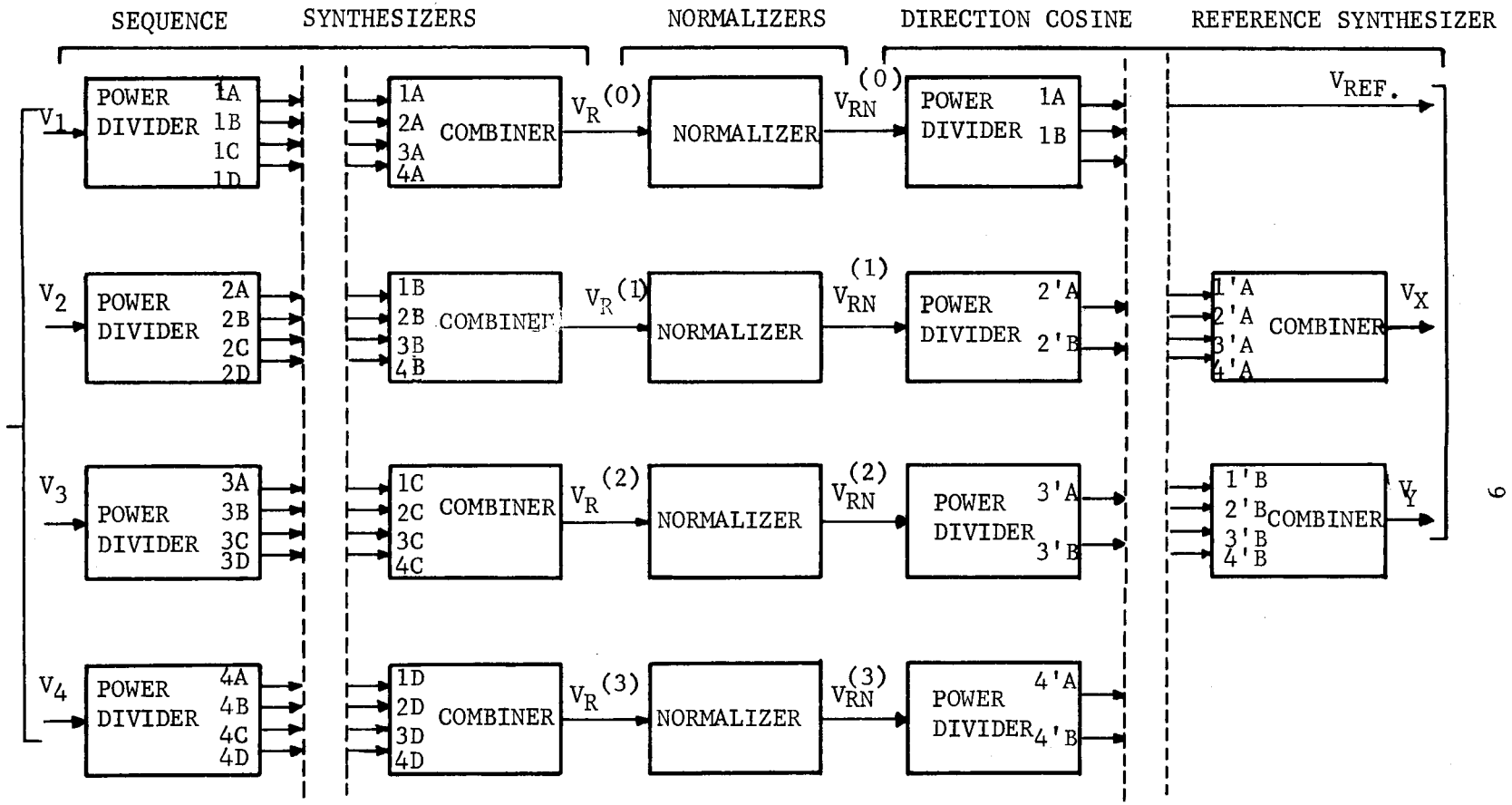

X	1A	2A	3A	4A	1B	1C	1D	3C	1'A	2A	3'A	4'A	1'B
X + λ/4	4B	2D	2B										
X + λ/2	3B	2C	4C	3D	3B								
X + 3λ/4	2B	4D	4B										

Figure 2--Radio Frequency Direction Finding System

III. An Operational Direction Finding Antenna

From the previous analysis, it is easily seen how direction information may be obtained by comparing the phase of V_1 and V_m with V_{Ref} for the hypothetical array of point sources. But an operational direction finding system must make use of elements other than point sources. Since the frequency of operation for this particular direction finding system is 138 M Hz (a wavelength over seven feet), the physical size of an efficient radiator at this frequency dictates that a linear type element must be used.

One basic requirement that an operational direction finding antenna must meet is to be able to receive a signal of any polarization. This is necessary because the antenna on the space vehicle is linearly polarized, but the attitude of the space vehicle may cause the transmitted signal to have any given polarization.

Linear elements, such as dipoles and monopoles, are linearly polarized; therefore, in order for the direction finding antenna to receive signals of any polarization, a combination of linear elements must be used.

A practical solution to the polarization problem is to employ a ring of horizontal elements and a ring of vertical elements with each ring independently fed. An antenna of this type will respond to any polarization, but it requires two direction cosine synthesis networks. The direction finding system will obviously need some kind of logic to decide whether the direction cosines should be derived

from the vertical or from the horizontal ring, but this can easily be accomplished by a threshold device in the direction finding system receiver.

For this particular system the radius of the circle on which the elements are to be positioned has been previously specified $\lambda/4$. As a result, the longest element that can be used in the horizontal ring is $\lambda/2$. Therefore, an excellent choice for the horizontal elements is a half-wavelength center-fed dipole.

Before deciding what element to use for the vertical ring, the problem of multipath signals, which introduce errors in direction cosine measurements, will be considered.

The performance of a phase measuring system is especially susceptible to multipath since it must measure the direction of the incoming signal. The greatest source of multipath signals is usually the ground surrounding the antenna. The magnitude of the multipath signal will vary with the reflection coefficient of the earth. Because of this variation in the earth's reflection coefficient, the antenna will perform better if it is built over a metallic ground plane with a constant reflection coefficient.

Since there will need to be other equipment in the vicinity of the direction finding antenna, it will be necessary to elevate the direction finding antenna in order to keep incoming signals from being blocked. From figure 3 it can be seen that the effects of the multipath signals will be inversely proportional to the height and size of the antenna's ground plane, and will be directly proportional to the height of the antenna above its ground plane.

From the above discussion on multipath degradation, it is obvious that a good choice for the vertical elements is a monopole with its terminal on the ground plane.

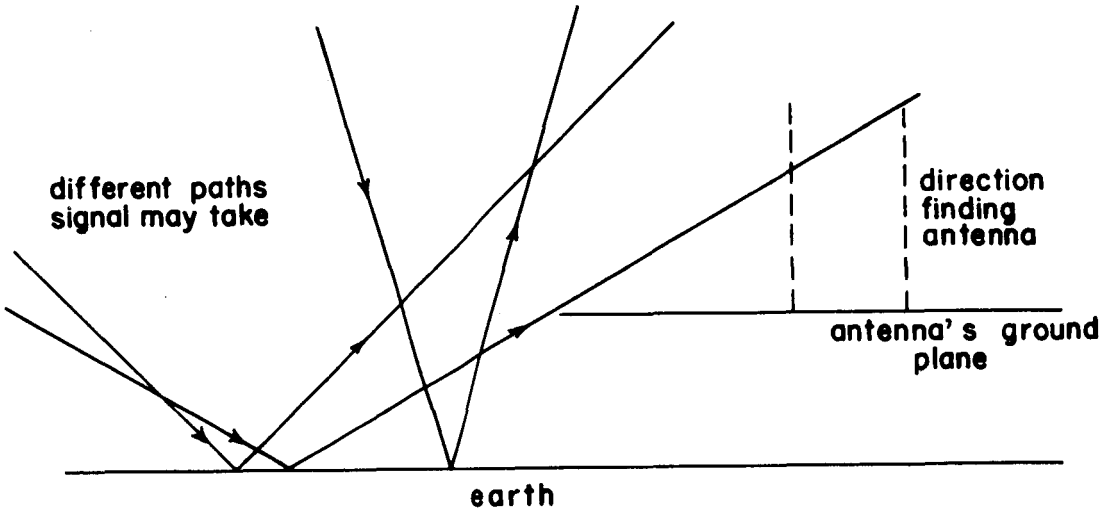

Figure 3--Effects of Ground Reflections on the Direction Finding Antenna.

Before deciding on the length of the vertical monopoles, other considerations of the properties of the direction finding antenna should be taken into account.

Since the vertical elements have a null in their pattern for $\Theta = 0^{o}$, it is necessary for the horizontal elements to be able to receive signals in the vicinity of $\Theta = 0^{o}$. For a horizontal dipole above a ground plane, the directional pattern is maximum at $\Theta = 0$ whenever the height of the dipole above the ground plane is $\lambda/4$ or less, as can be seen from figure 4.

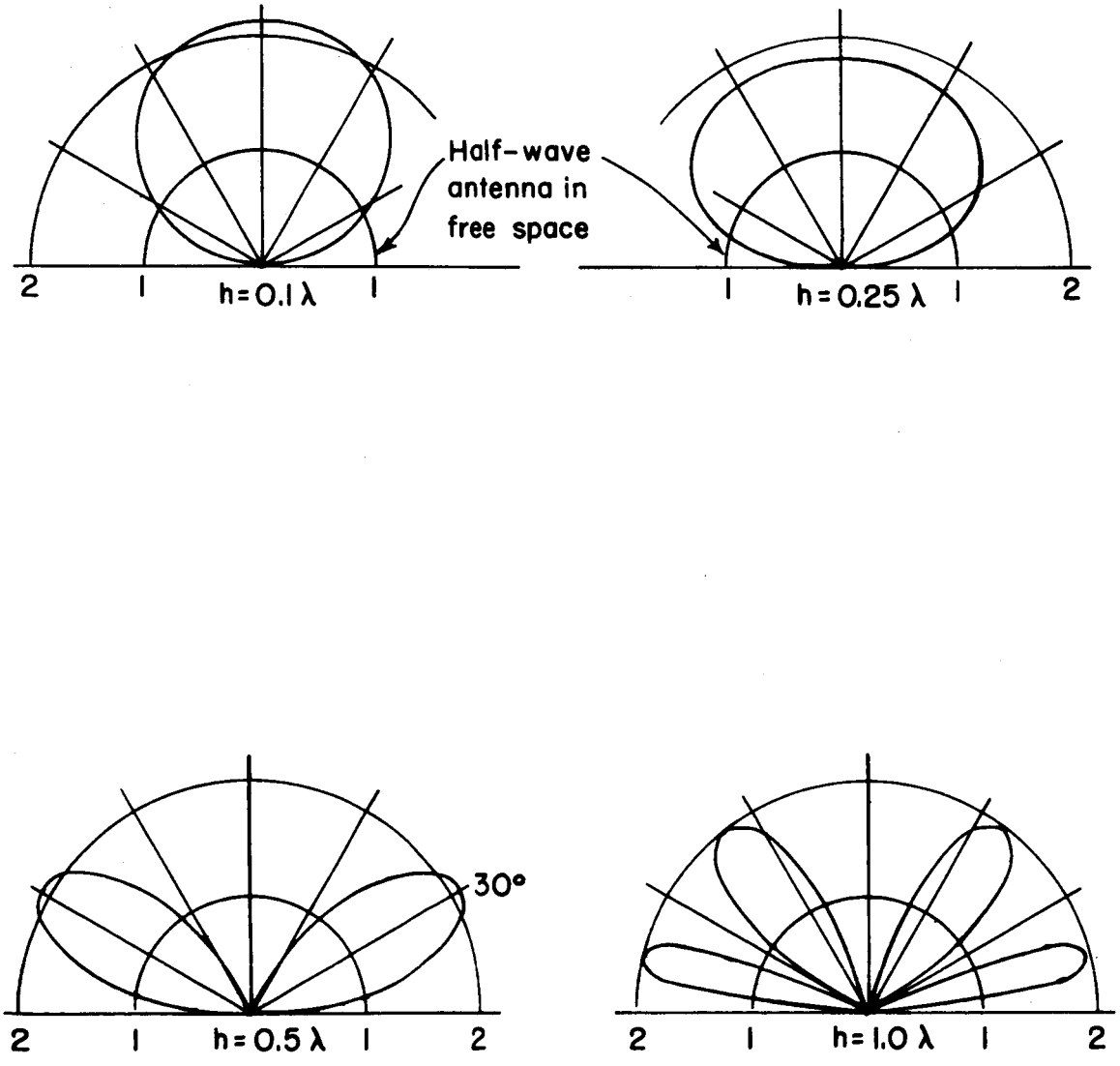

Figure 4--Radiation Patterns of a λ/4 Dipole
for Different Heights Above a Ground Plane.

Also, for $h = \lambda/4$ the relative field strength is greater in the vicinity of $\theta = \pi/2$ than when $h < \lambda/4$; therefore, $h = \lambda/4$ would be a better choice than some $h < \lambda/4$ for receiving horizontally polarized signals along the horizon.

Another reason for choosing $h = \lambda/4$ is the ease with which both vertical and horizontal elements can be fed. Since coaxial cables will be used in the direction cosine synthesis network, and since dipoles must be fed from a balanced line, some type of balun will be needed for feeding the dipoles. If a "bazooka" balun is used, then the balun can also be used for one of the elements of a vertical folded monopole. This configuration is shown in figure 5.

Since the elements are perpendicular to each other, they do not interact. That is, the mutual impedance between horizontal and vertical elements is essentially zero. Therefore, the equations for V_1, V_m, and V_{Ref} of the vertical elements will be independent of the horizontal elements, and vice-versa. Moreover, because the horizontal and vertical rings are isolated, the equations for V_1, V_m, and V_{Ref} will be the same as for the array of point sources; but, for the operational direction finding system, the $f_i(\theta,\phi)$ will have to be substituted in the equations.

For the vertical ring, the $\lambda/4$ folded monopole has the same directional pattern as a single $\lambda/4$ monopole. Their pattern [2] is

$$f_i(\theta,\phi) = f_i(\theta) = \frac{\cos(\pi/2 \cos\theta)}{\sin\theta} \text{ [2] , where}$$

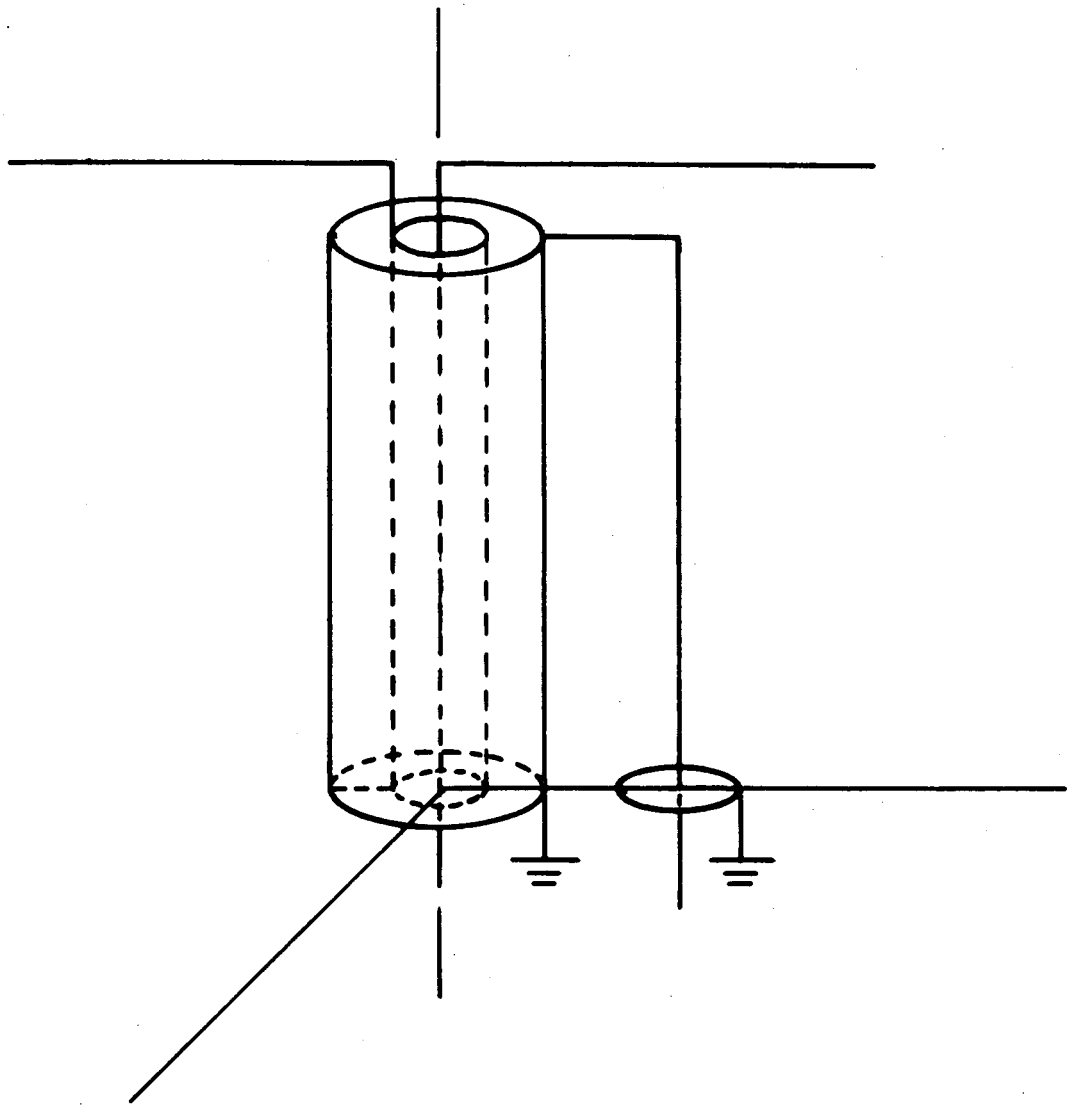

Figure 5--An illustration of a monopole-dipole radiating element.

Θ is measured from the antenna's axis.

For Θ polarization, V_l, V_m and V_{Ref} for the vertical ring become

$$V_l = \frac{4 \cos(\pi/2 \cos \Theta)}{\sin \Theta} e^{-jcl}$$

$$V_m = \frac{4 \cos(\pi/2 \cos \Theta)}{\sin \Theta} e^{-jcm}$$

$$V_{Ref} = \frac{2 \cos(\pi/2 \cos \Theta)}{\sin \Theta} [\cos cl + \cos cm] \quad .$$

The vertical elements will not respond to Φ-polarization and V_l, V_m, and V_{Ref} will all be zero for Φ-polarization.

From figure 6 it can be seen, that for some polarization other than Θ or Φ, the voltages will vary as $|\cos \alpha|$, where α is the angle between the unit vector in the Θ direction, and E (the electric field vector).

Therefore, V_l, V_m, and V_{Ref} for any polarization can be written:

$$V_{,v} = 4 |\cos \alpha| \frac{\cos[\pi/2 \cos \Theta]}{\sin \Theta} e^{-jcl}$$

$$V_{m,v} = 4 |\cos \alpha| \frac{\cos[\pi/2 \cos \Theta]}{\sin \Theta} e^{-jcm} \qquad (8)$$

$$V_{Ref,v} = 2 |\cos \alpha| \frac{\cos[\pi/2 \cos \Theta]}{\sin \Theta} [\cos cl + \cos cm] ,$$

where the subscript v denotes the vertical ring.

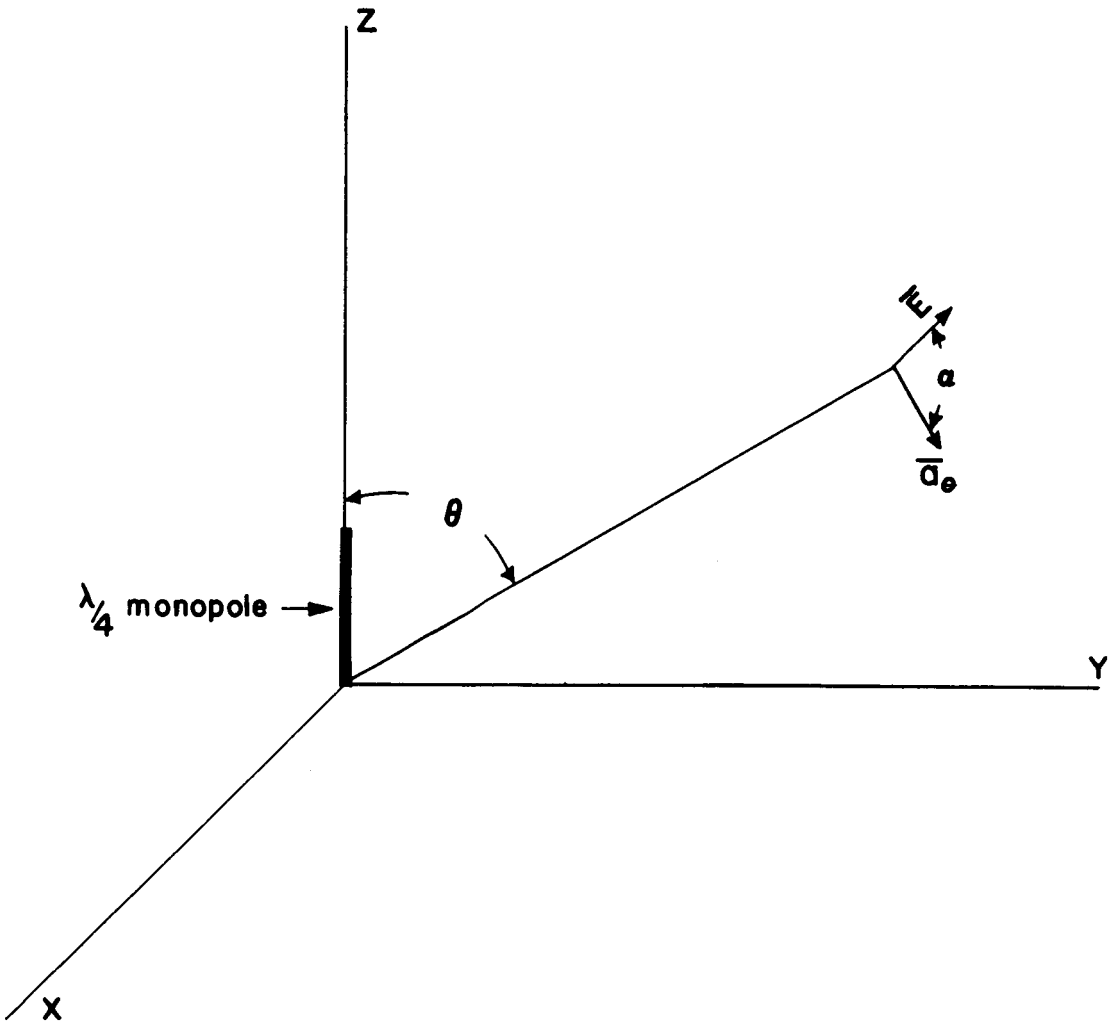

Figure 6--Coordinate System for the Vertical Monopoles.

For the horizontal ring, the horizontal elements and their images will appear as in figure 7.

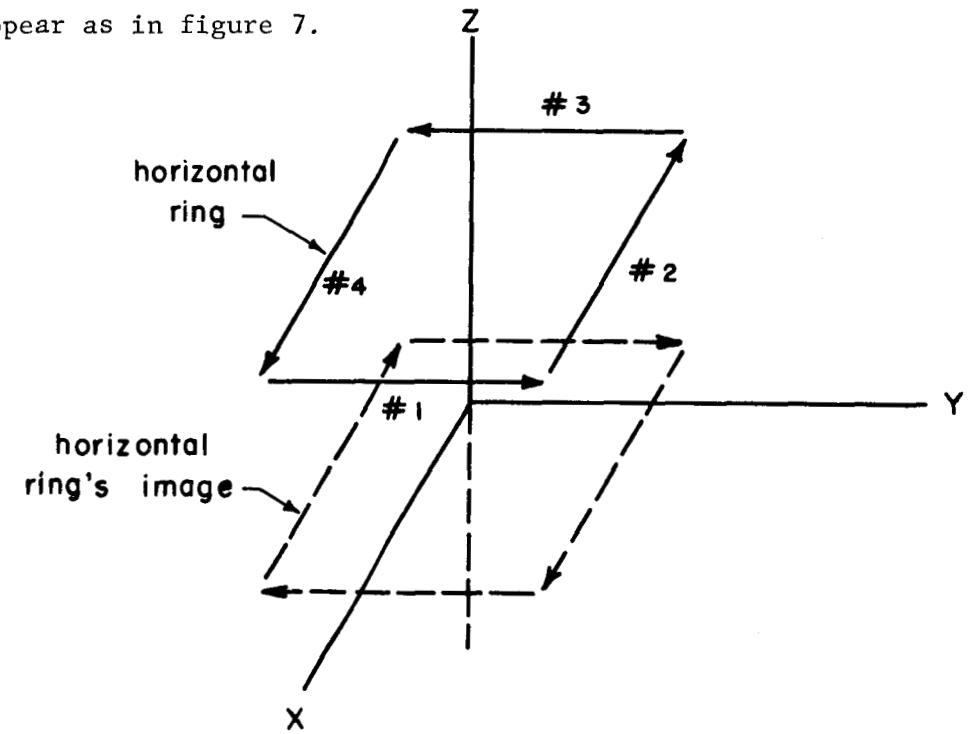

Figure 7--Horizontal Ring of Dipoles and Its Image

Each element and its image is a two element array with the elements 180° out of phase. The point where the axis of the two element array intersects the ground plane will be taken as the phase reference of the two element array. The $f_i(\Theta,\Phi)$ terms in the expressions for V_1 V_m, and V_{Ref} will be the product of the element's pattern factor and the pattern factor of two point sources located at the element and its image.

The $\lambda/2$ dipole in figure 8 has an element factor given by

$$F(\Theta_x) = |\cos \beta_1| \quad \frac{\cos[\pi/2 \cos \Theta_x]}{\sin \Theta_x} \quad .$$

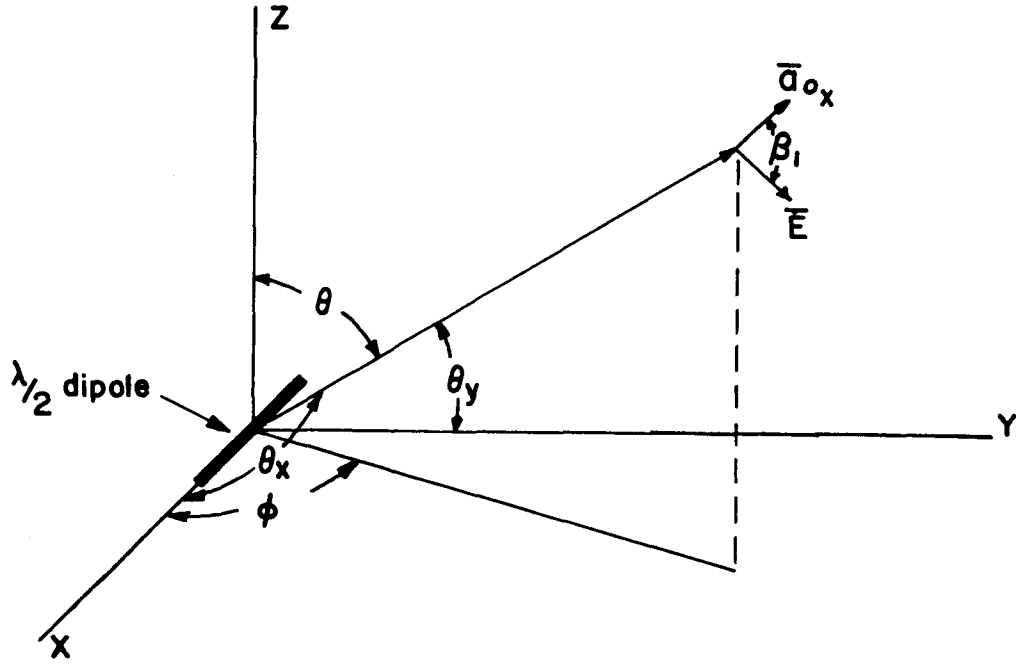

Figure 8--Coordinate System for a Dipole Along the X-Axis.

The term $|\cos \beta_1|$ is included to take into account polarizations other than those in the $\bar{a}_{\theta_x}$ direction.

Also, from figure 8 , it can be seen that $\cos \theta_x = \sin \theta \cos \phi$, which yields

$$F(\theta,\phi) = |\cos \beta_1| \frac{\cos[\pi/2 \sin \theta \cos \phi]}{\sqrt{1 - \sin^2 \theta \cos^2 \phi}} . \quad (9)$$

Elements 2 and 4 of the horizontal ring will have an element factor as in (9).

The $\lambda/2$ dipole in figure 9 has an element factor given by

$$F(\theta_y) = |\cos \beta_2| \frac{\cos [\pi/2 \cos \theta_y]}{\sin \theta_y} .$$

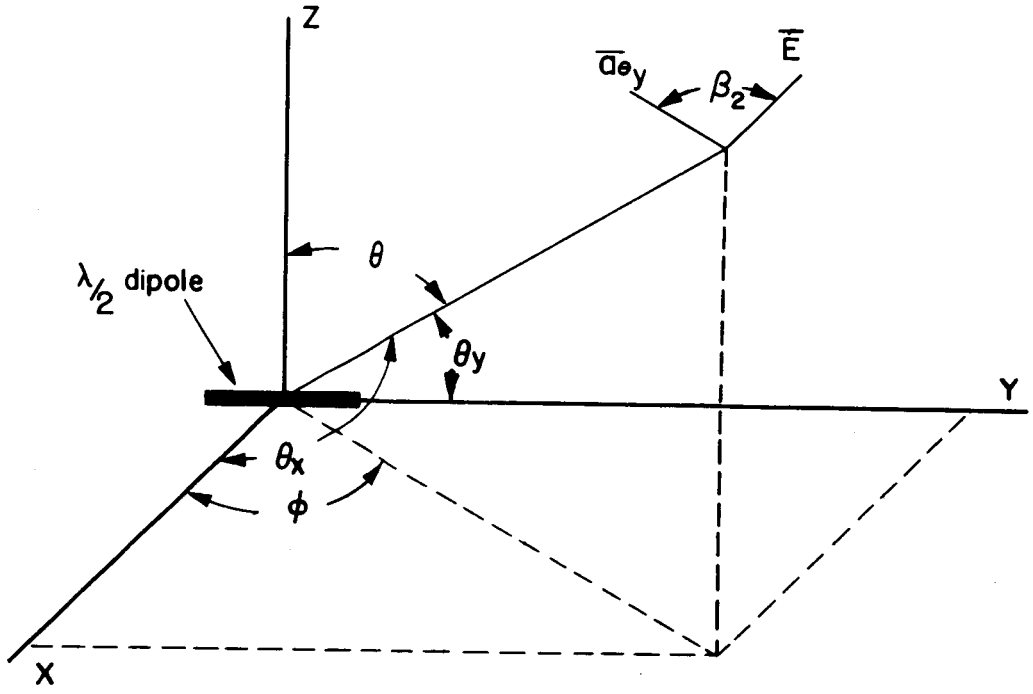

Figure 9--Coordinate System for a Dipole Along the Y-Axis.

The term $|\cos\beta_2|$ encompasses polarizations other than those in the $\bar{a}_{\theta y}$ directions, Now

$\cos \theta_y = \sin \theta \sin \phi$ and

$$F(\theta,\phi) = |\cos \beta_2| \frac{\cos[\pi/2 \sin \theta \sin \phi]}{\sqrt{1 - \sin^2 \theta \sin^2\phi}} . \qquad (10)$$

Elements 1 and 3 of the horizontal ring will have element factors as in (10).

The pattern factor for the two element array of point sources for all four elements is the same, and is given by

$$2 \sin [\pi/2 \cos \theta] \quad .$$

Therefore,

$$f_1(\theta,\phi) = f_3(\theta,\phi) = \frac{2\,|\cos \beta_2| \sin [\pi/2 \cos \theta] \cos[\pi/2 \sin \theta \sin \phi]}{\sqrt{1 - \sin^2 \theta \sin^2 \phi}} \quad ,$$

and

$$f_2(\theta,\phi) = f_4(\theta,\phi) = \frac{2|\cos \beta_1| \sin[\pi/2 \cos \theta] \cos [\pi/2 \sin \theta \cos \phi]}{\sqrt{1 - \sin^2 \theta \cos^2 \phi}} \quad .$$

It is important to know the angle between $\bar{a}_{\theta y}$ and $\bar{a}_{\theta x}$ for different θ and ϕ. This angle will be called β and $\beta = \beta_2 - \beta_1$.

Both the unit vectors $\bar{a}_{\theta x}$ and $\bar{a}_{\theta y}$ will always be in a plane that is orthogonal to the radial vector $\bar{r}$. $\bar{a}_{\theta x}$ will be in the plane which passes through the x-axis and the radial vector $\bar{r}$. $\bar{a}_{\theta y}$ will be in the plane which passes through the y-axis and the radial vector $\bar{r}$. The angle β is also the angle between these two planes, and, since the angle between two planes is defined [3] as the angle between their normals, β can be found by finding normal vectors to each plane and by solving for the angle between them.

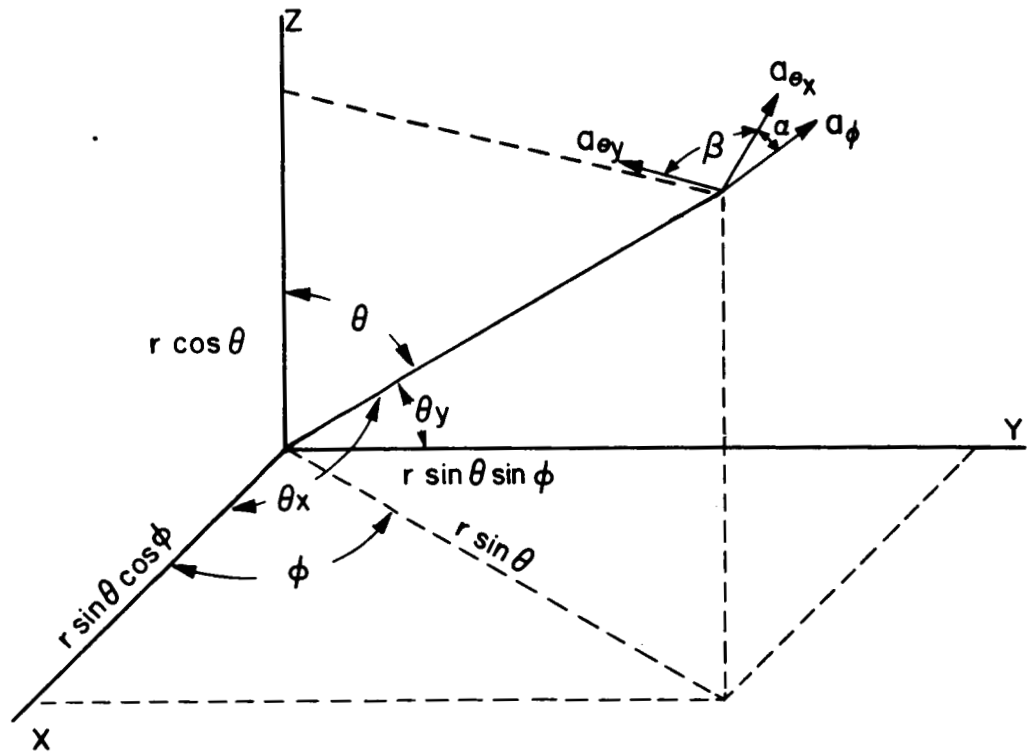

Figure 10--The Coordinate System Used for Calculating β_1 and β_2.

From figure 10 we see that $\bar{r}$ can be written in cartesian coordinates as

$$\bar{r} = |\bar{r}| \sin\Theta \cos\Phi\, \bar{i} + |\bar{r}| \sin\Theta \sin\Phi\, \bar{j} + |\bar{r}| \cos\Theta\, \bar{k}.$$

If we let a vector in the x direction be $A\bar{i}$, then we can find a vector normal to the plane containing the x-axis and $\bar{r}$ by taking the cross-product of $A\bar{i}$ and $\bar{r}$. This normal vector $\bar{N}_x$ is found to be

$$\bar{N}_x = A\,|\bar{r}|\,\sin\theta\,\sin\phi\,\bar{k} - A\,|\bar{r}|\,\cos\theta\,\bar{j}\ .$$

Similarly, if we let a vector in the y direction be $B\bar{j}$, then we find $\bar{N}_y$, a vector normal to the plane containing the y-axis and $\bar{r}$, to be

$$\bar{N}_y = B|\bar{r}|\,\cos\theta\,\bar{i} - B\,|\bar{r}|\,\sin\theta\,\cos\phi\,\bar{k}\ .$$

The angle β can be found by taking the dot product of $\bar{N}_x$ and $\bar{N}_y$,

$$\bar{N}_x \cdot \bar{N}_y = |\bar{N}_x|\ |\bar{N}_y|\ \cos\beta$$

$$\cos\beta = \frac{\bar{N}_x \cdot \bar{N}_y}{|\bar{N}_x|\ |\bar{N}_y|} = \frac{-\sin^2\theta\,\cos\phi\,\sin\phi}{\sqrt{\cos^2\theta + \sin^2\theta\,\sin^2\phi}\sqrt{\cos^2\theta + \sin^2\theta\,\cos^2\phi}}\ . \tag{11}$$

Now the equation for V_1, V_m, and V_{Ref} of the horizontal ring are

$$V_{1h} = 4\,f_1(\theta,\phi)e^{-jc\,l} = \frac{8|\cos\beta_2|\sin[\pi/2\,\cos\theta]\,\cos[\pi/2\,\sin\theta\,\sin\phi]}{\sqrt{1 - \sin^2\theta\,\sin^2\phi}}\,e^{-\,jc\,l}$$

$$V_{mh} = 4\,f_4(\theta,\phi)e^{-jcm} = \frac{8|\cos\beta_1\,|\sin[\pi/2\,\cos\theta]\,\cos[\pi/2\,\sin]\,\cos\phi]}{\sqrt{1 - \sin^2\theta\,\cos^2\phi}}\,e^{-jcm}$$

$$V_{Refh} = f_1(\theta,\phi)[e^{-jcl} + e^{jcl}] + f_2(\theta,\phi)\,[e^{-jcm} + e^{jcm}] \tag{12}$$

$$= \frac{4 \cos cl\ |\cos \beta_2|\ \sin[\pi/2 \cos\theta]\ \cos[\pi/2 \sin\theta \sin\phi]}{\sqrt{1 - \sin^2\theta \sin^2\phi}}$$

$$+ \frac{4 \cos cm\ |\cos \beta_1|\ \sin[\pi/2 \cos\theta]\ \cos[\pi/2 \sin\theta \cos\phi]}{\sqrt{1 - \sin^2\theta \cos^2\phi}} .$$

Because of certain isolated cases when the voltages in (8) and (12) are zero, some kind of logic must be used to obtain correct direction information. Inspection of equations (8) and (12) reveals that $V_{l,v}$, $V_{m,v}$, and $V_{Ref,v}$ are all zero when $\theta=0$, and $V_{m,h}$ $V_{l,h} = 0$ when both β_1 and β_2 are $\pi/2$. Because of the absence of signal at $\theta = 0$ for this case, no phase measurements could be made, but when $\theta = 0$ both $\cos \theta_x$ and $\cos \theta_y$ are zero. This allows the logic system used to decide that both the direction cosines are zero when there is no signal from both the vertical and horizontal rings.

IV. Analysis and Optimization of the Feed System and Individual Antenna Elements

To obtain optimum performance from a direction finding system, certain aspects of the antenna feed system and antenna elements should be taken into consideration.

A. The D. F. Feed System

The feed system for the direction finding system synthesizes the voltages from which direction information is derived. The feed system consists of phased transmission lines (coaxial type), power dividers and summers, and attenuators. To understand the feed system fully, an analysis of the device used as a power divider and summer is necessary. Since the two-way, three-way, and four-way power dividers and summers (hereafter called multicouplers) function similarly, an analysis of the two-way multicoupler is sufficient.

1. Power Dividers and Summers

From figure 11 it can be seen that the two-way multicouplers consist of two $\lambda/4$ transmission lines with characteristic impedance of 70.7 ohms connected in parallel at port 1. At ports 2 and 3 an 100 ohm isolation resistor is connected between the center conductors of ports 2 and 3.

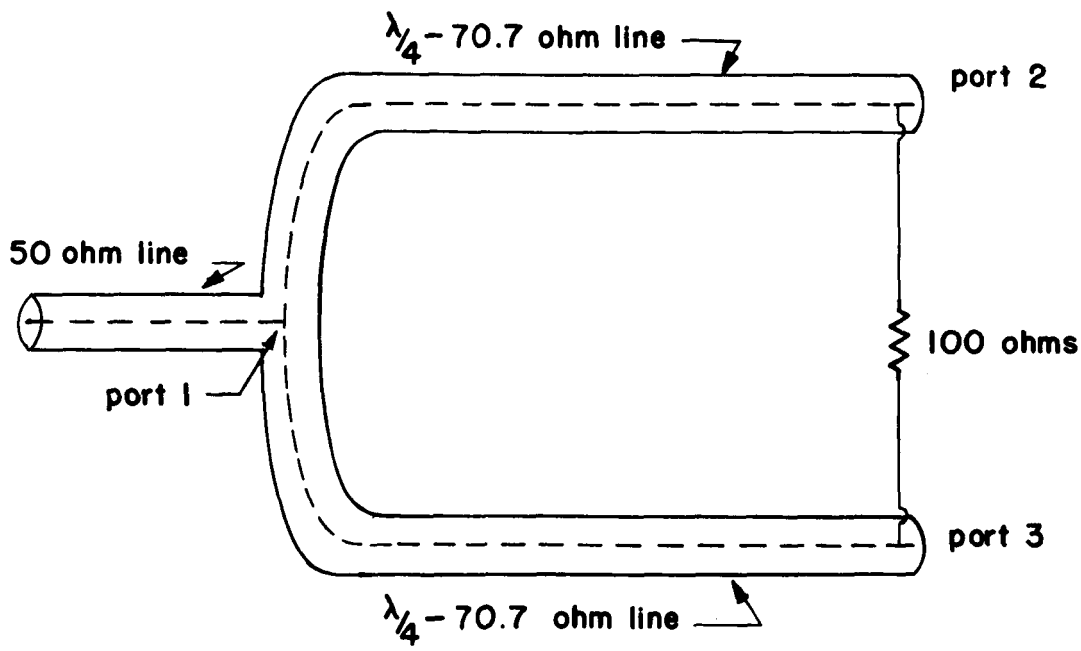

Figure 11--Illustration of the Two-Way Multicoupler.

To understand how isolation between ports 2 and 3 is obtained, consider the situation when power at the operating frequency is applied to port 2. At port 2 the power is divided between the 100 Ω resistor and the 70.7 Ω transmission line. At port 3 the signal in the 70.7 Ω lines is approximately 180° out of phase with the

signal in the isolation resistor, and when the two signals combine partial cancellation is achieved.

In order to describe other features of the multicoupler thoroughly, the distributed parameters of the transmission lines can be resolved into lumped parameters through transmission line techniques, and the equivalent circuit for the two-way multicoupler can be drawn as in figure 12.

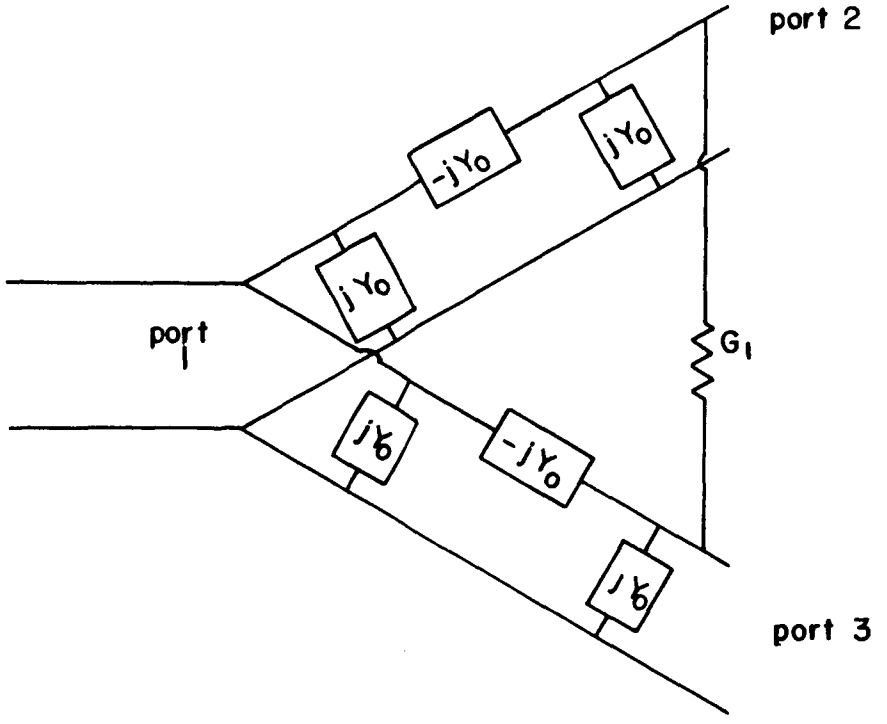

Figure 12--Schematic Diagram of the Two-Way Multicoupler.

In figure 12 all parameters are admittances with Y_o the characteristic admittance of the $\lambda/4$ transmission lines.

The circuit can be redrawn as in figure 13 to assist in writing the equations for the multicoupler.

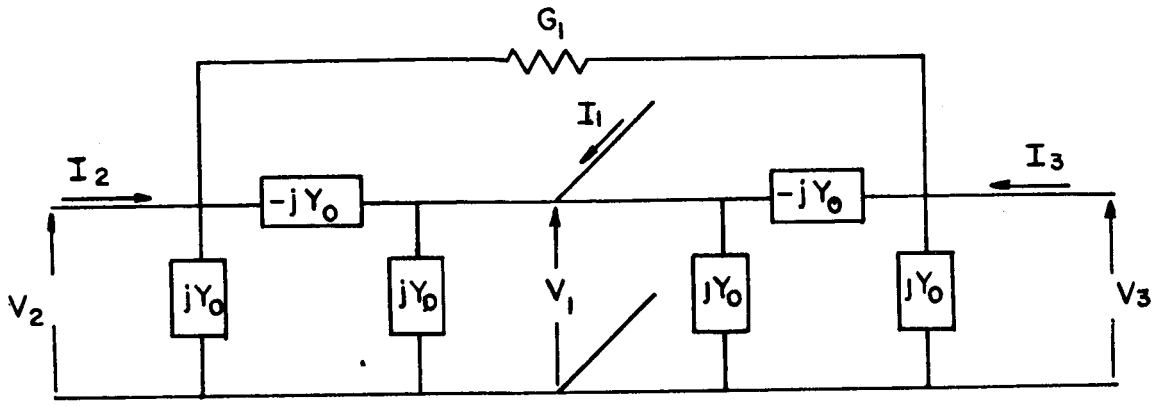

Figure 13--Simplified Schematic Diagram of the Two-Way Multicoupler.

The steady-state equations for the circuit in figure 13 are:

$$\begin{bmatrix} I_1 \\ I_2 \\ I_3 \end{bmatrix} = \begin{bmatrix} 0 & jY_o & jY_o \\ jY_o & G_1 & -G_1 \\ jY_o & -G_1 & G_1 \end{bmatrix} \begin{bmatrix} V_1 \\ V_2 \\ V_3 \end{bmatrix} . \qquad (13)$$

When the multicoupler is used as a power summer, we will be interested in the voltage V_1 with port 1 terminated in G due to I_1 and I_2.

When port 1 is terminated in G, equations (13) become

$$\begin{bmatrix} 0 \\ I_2 \\ I_3 \end{bmatrix} = \begin{bmatrix} G & jY_o & jY_o \\ jY_o & G_1 & -G_1 \\ jY_o & -G_1 & G_1 \end{bmatrix} \begin{bmatrix} V_1 \\ V_2 \\ V_3 \end{bmatrix} \quad . \tag{14}$$

Solving (14) for V_1 we find that

$$V_1 = \frac{-j}{2Y_o} [I_2 + I_3] \quad .$$

It is important to note, that the equation for V_1 has the same form as the sequence voltages; that is, the sum of currents across a common load. Therefore, the multicoupler will function properly in synthesizing the sequence voltages.

One undesirable characteristic of this particular multicoupler is that when there is a potential across the isolation resistor, current will flow in the resistor and power will be dissipated.

$$P_L=(1/2)(V_2-V_3)^2G_1,$$

and, solving (13) for V_2 and V_3, we find

$$P_L = \frac{[I_2 - I_3]^2}{8G_1} \quad . \tag{15}$$

From (15) it can be concluded that there is no power dissipated in G_1 when I_2 and I_3 are equal in magnitude and are in phase, but

whenever I_2 and I_3 are not equal, P_L is proportional to the square of their difference.

For determining the impedance looking into port three, the circuit is shown in figure 14,

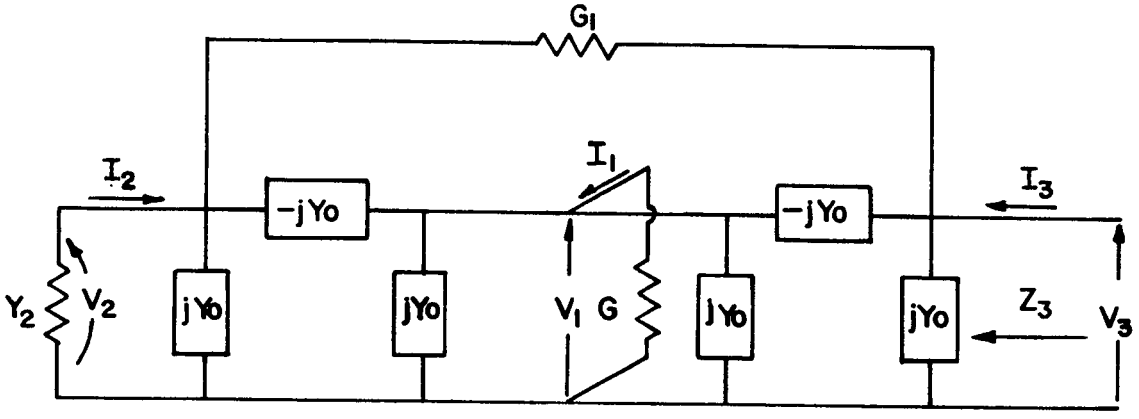

Figure 14--Schematic Diagram for Determining Z_3 of the Two-Way Multicoupler.

and the equations become,

$$\begin{bmatrix} 0 \\ 0 \\ I_3 \end{bmatrix} = \begin{bmatrix} G & jY_o & jY_o \\ jY_o & G_1+G_2 & -G_1 \\ jY_o & -G_1 & G_1 \end{bmatrix} \begin{bmatrix} V_1 \\ V_2 \\ V_3 \end{bmatrix} . \qquad (16)$$

Solving (16) for V_3 we obtain

$$V_3 = I_3 \frac{[GG_1 + GG_2 + Y_o^2]}{\Delta} \text{ , where } \Delta = 4G_1Y_o^2 + GG_1G_2 + G_2Y_o^2$$

$$Z_3 = \frac{V_3}{I_3} = \frac{GG_1 + GG_2 + Y_o^2}{4G_1Y_o^2 + GG_1G_2 + G_2Y_o^2} \quad .$$

If matched conditions are assumed (i.e., ports 1 and 2 terminated in 50 ohms), then $Z_3 = 50$. To find out how Z_3 varies for different loads, Z_3 can be differentiated with respect to G_2 and G:

$$\frac{dZ_3}{dG_2} = \frac{[4G_1Y_o^2+G_1GG_2+G_2Y_o^2]G-[GG_1+GG_2+Y_o^2][Y_o^2+GG_1]}{[4G_1Y_o^2 + GG_1G_2 + G_2Y_o^2]^2}$$

$$= -\frac{[GG_1 - Y_o^2]^2}{[4G_1Y_o^2 + GG_1G_2 + G_2Y_o^2]^2} \quad \text{and since } Y_o = 2\,G_1$$

$$\frac{dZ_3}{dG_2} = -\frac{[G_1(G - 2G_1)]^2}{D} \quad .$$

For the case when G is $20X10^{-3}$ mhos, $\frac{dZ_3}{dG_2} = 0$ and the impedance looking into port 3 is independent of G_2. But, when port 1 is not terminated with a matched load, Z_3 will vary with G_2.

Since the multicoupler is symmetrical, the input impedance of port 2 will be the same as Z_3.

To find the input impedance at port 1, the circuit is shown in figure 15, and $Z_1 = \frac{V_1}{I_1}$.

From the expression for Z_1, we find that $Z_1 = 50$ when matched conditions exist (i.e., when ports 2 and 3 are terminated in 50 ohms).

To discover how Z_1 varies with Y_2 and Y_3, Z_1 can be differentiated with respect to Y_2 or Y_3. Since the multicoupler is symmetrical, investigation of Z_1's variance with Y_2 is sufficient:

$$\frac{dZ_1}{dY_2} = \frac{[2G_1 + Y_3]^2}{Y_o^2(4G_1 + Y_2 + Y_3)^2} \quad . \tag{16}$$

From (16) it can be seen that $\frac{dZ_1}{dY_2}$ will never be zero, since G_1 is real and positive, and whenever Y_3 is purely real it will also be positive.

2. Normalization of the Sequence Voltages

Inspection of equations (3) reveals that the sequence voltages do not have the same magnitude and phase. This difference would cause V_1 and V_m to be synthesized incorrectly. The difference in magnitude and phase results from the sequence impedances, which are combinations of self and mutual impedances of the antenna elements. Since accurate values for the mutual impedances of elements oriented like the ones used in the direction finding array are not available, an experimental method of normalization is needed.

a. Vertical Ring

The magnitude of the sequence voltages will be normalized first, and then the phase of the sequence voltages will be dealt with.

From equations (3) we noted that

$$V^{(0)} = \frac{VR}{|Z^{(0)}|} e^{-j\phi_0} \left[f_1(\theta,\phi)e^{-jc1} + f_2(\theta,\phi)e^{-jcm} + f_3(\theta,\phi)e^{jc1} + f_4(\theta,\phi)e^{jcm} \right]$$

the $f_i(\theta,\phi)$ for the vertical folded monopoles are all the same, and are independent of ϕ. Therefore,

$$|V^{(0)}| = \frac{|VR|}{|Z^{(0)}|} |f_1(\theta,\phi)| \; |e^{-jc1} + e^{-jcm} + e^{jc1} + e^{jcm}| \; ,$$

where $c1 = -ka \sin\theta \cos\phi$ and $cm = -ka \sin\theta \sin\phi$.

If we let $\theta = \pi/2$ and $\phi = 0$, we have

$$|f_1(\theta,\phi)| = 1$$

$$c1 = -ka = -\left(\frac{2\pi}{\lambda}\right)\left(\lambda/4\right) = -\pi/2, \text{ and } cm = 0.$$

This yields:

$$|V^{(0)}| = 2 \; \frac{|VR|}{|Z^{(0)}|} \; .$$

If the same conditions are applied to the other sequence voltages, we find

$$|V^{(1)}| = 2 \frac{|VR|}{|Z^{(1)}|}$$

$$|V^{(2)}| = 2 \frac{|VR|}{|Z^{(2)}|}$$

$$|V^{(3)}| = 2 \frac{|VR|}{|Z^{(3)}|} \quad .$$

From the equations above, it can be seen that the only terms that are different in the equations for the magnitudes of the sequence voltages are the respective sequence impedances. Therefore, if the antenna is oriented so that $\Theta = \pi/2$ and $\Phi = 0$, and the sequence voltages are measured, comparison of the relative amplitudes of the sequence voltages will enable the voltages to be normalized. In other words, the sequence voltage which has the smallest magnitude can be chosen as the reference and the other voltages can be attenuated until they equal the reference voltage.

After the sequence voltage's magnitudes have been normalized, the sequence voltages are

$$V^{(o)} = e^{-j\phi_o} f_1(\Theta,\Phi)[e^{-jcl} + e^{-jcm} + e^{jcl} + e^{jcm}]$$

$$V^{(1)} = e^{-j\phi_1} f_1(\Theta,\Phi)[e^{-jcl} + je^{-jcm} - e^{jcl} - je^{jcm}]$$

$$V^{(2)} = e^{-j\phi_2} f_1(\Theta,\Phi)[e^{-jcl} - e^{-jcm} + e^{jcl} - e^{jcm}]$$

$$V^{(3)} = e^{-j\phi 3} f_1(\theta,\phi)[e^{-jc1} - je^{-jcm} - e^{jc1} + je^{jcm}] \quad .$$

If we again let $\theta = \pi/2$ and $\phi = 0$, the voltages become

$$V^{(o)} = 2e^{-j(\phi_o)}$$

$$V^{(1)} = 2e^{-j(\phi_1-90^o)}$$

$$V^{(2)} = 2e^{-j(\phi_2-180^o)}$$

$$V^{(3)} = 2e^{-j(\phi_3-90^o)} \quad .$$

Therefore, with the antenna oriented so that $\theta = \pi/2$ and $\phi = 0$, the amount of phase that should be added to each voltage can be found by measuring the phase of the sequence voltages with respect to some reference phase, and then comparing the relative phase associated with each sequence impedance.

The phase shift required for normalizing the sequence voltages can be accomplished by inserting the correct length of transmission line.

b. Horizontal Ring

The procedure for normalizing the sequence voltages of the horizontal ring is similar to the procedure for the vertical ring, but is more complicated because the $f_i(\theta,\phi)$ are not independent of ϕ. A position must be chosen for transmitting so that none of the sequence voltages are zero. A good choice for this position is $\theta = 45^o$ and $\phi = 45^o$. With these values of θ and ϕ we obtain

c 1 = $-\pi/4$ and cm = $-\pi/4$, and from equations (3) the sequence voltages become:

$$V^{(o)} = \frac{VR}{|Z^{(o)}|} e^{-j\phi_o} [1.02 |\cos \beta_2| + 1.02 | \cos \beta_1|]$$

$$V^{(1)} = \frac{VR}{|Z^{(1)}|} e^{-j\phi_1} [j1.02 |\cos \beta_2 | - 1.02 | \cos \beta_1 |]$$

$$V^{(2)} = \frac{VR}{|Z^{(2)}|} e^{-j\phi_2} [1.02 |\cos \beta_2 | - j1.02 | \cos \beta_1 |]$$

$$V^{(3)} = \frac{VR}{|Z^{(3)}|} e^{-j\phi_3} [j1.02 |\cos \beta_2 | - j1.02 | \cos \beta_1|] .$$

If we orient the transmitting antenna so that $\beta_1 = 90^o$, we find from equation (11) that $\beta_2 = 160.5^o$ and the sequence voltages become:

$$V^{(o)} = \frac{.96VR}{|Z^{(o)}|} e^{-j\phi_o}$$

$$V^{(1)} = \frac{j.96VR}{|Z^{(1)}|} e^{-j\phi_1}$$

$$V^{(2)} = \frac{j.96VR}{|Z^{(2)}|} e^{-j\phi 1}$$

$$V^{(3)} = \frac{j.96\ VR}{|Z^{(3)}|} e^{-j\phi 3}$$

Now, by a procedure analagous to the procedure used for the vertical ring, the sequence voltages for the horizontal ring can be normalized in magnitude and phase.

C. Attenuators

The attenuators needed to normalized the sequence voltages in magnitude must meet two specifications: (1) the specified amount of attenuation, and (2) the correct matching impedance to the transmission lines feeding and terminating it.

The specifications can be met by a simple resistive attenuator in a T configuration, as shown in figure (16), if the correct resistors are chosen.

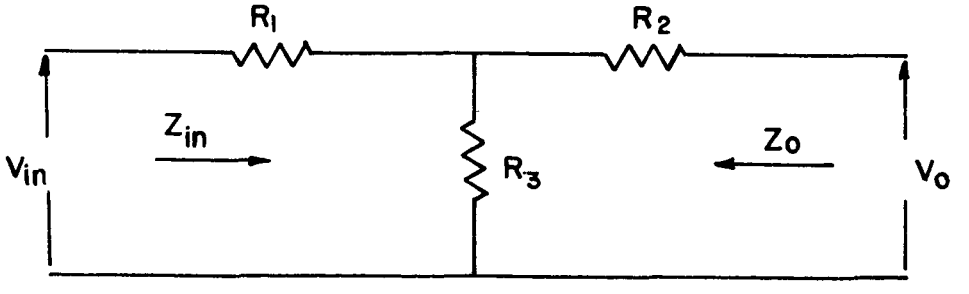

Figure 16--Schematic Diagram of an Attenuator in the T-Configuration.

Since the attenuators will be fed and terminated by 50 ohm transmission lines, $Z_{in} = Z_o$, which implies that $R_1 = R_2$. The correct values for R_1 and R_3 can be found by solving for Z_{in} and $N = \frac{V_o}{V_{in}}$; hence:

$$Z_{in} = \frac{(Z_o + R_1)\, R_3}{Z_o + R_1 + R_3} + R_1 .$$

Therefore,

$$Z_o = \frac{(Z_o + R_1)\, R_3}{Z_o + R_1 + R_3} + R_1, \text{ which implies that}$$

$$R_1^2 + 2R_1R_2 - R_o^2 = 0 . \tag{17}$$

Solving for N we find that

$$N = \frac{R_3}{R_1 + R_3 + Z_o} . \tag{18}$$

By rearranging equations (17) and (18), we find that if the required specifications are to be met, then

$$R_1 = \frac{Z_o(N - 1)}{N+1}$$

and

$$R_3 = 2\ R_o\left(\frac{N}{N^2-1}\right) .$$

B. Horizontal Dipole

A balanced transmission line is necessary for feeding the dipoles. For reasons already discussed, the "bazooka" balun will be used to transform the unbalanced coaxial cable into a balanced feed for the dipoles.

With the aid of figure (17), the operation of the balun can be understood by considering the situation that exists when a voltage is applied to the coaxial line from the dipole.

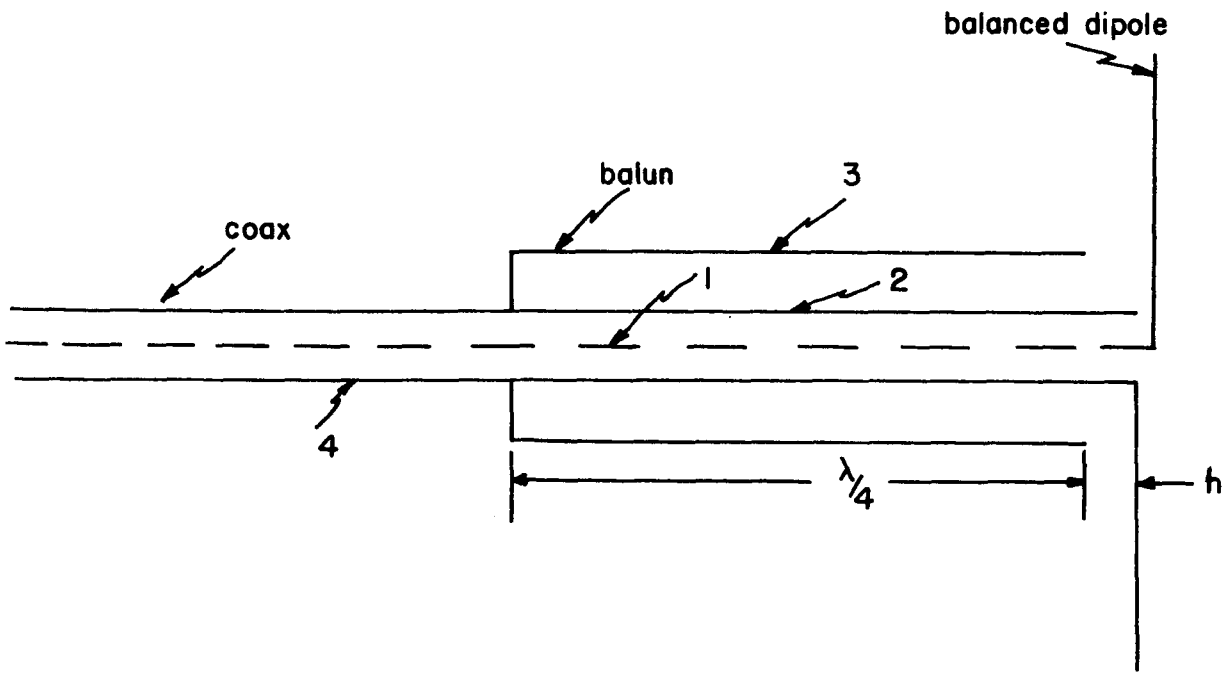

Figure 17--Illustration of the Balanced Feed for the Horizontal Dipole.

Since the voltage is applied across the conductors 1-2 of the coaxial line, it is transferred to the coaxial system without change. At the same time, the fact that 2 is an extension of the outer conductor, 4 of the coaxial system does not introduce an unbalance in the balanced system at 2 because, when the balun is exactly a quarter wavelength long, the impedance across 2-3 approaches infinity. That is, sleeve 3 acts as an extension of 4 and remains at the ground potential, whereas point 2 is free to assume any potential, the balanced system desires it to have.

It is very important that the dipole be balanced because the dipole's pattern will be unsymmetrical if it is not. The asymmetry would cause the signal received by different elements to be unequal, resulting in power being lost in the isolation resistors of the multicouplers. Therefore, it is important to choose the optimum distance h in figure 17.

An experimental setup was constructed, and antenna patterns and impedance measurements were recorded for various distances h. From the experimental results it can be seen that the dipole performs as desired until h becomes very large.

C. Vertical Folded Monopole

Since the magnitude of the signals used to derive the direction information is very small, it is important that the antennas transfer as much power as possible to the transmission lines. A problem with a folded monopole of unequal elements is that when the ratio of element diameters is large, there is a large impedance step-up that results

in a sizeable mismatch with the 50 ohm transmission lines. But, if the bridge connecting the elements is moved closer to the antenna's terminals, a decrease in the impedance step-up can be obtained. In light of this, the impedance of a folded monopole of unequal elements with a movable bridge will be investigated.

The antenna being investigated is shown in figure 18.

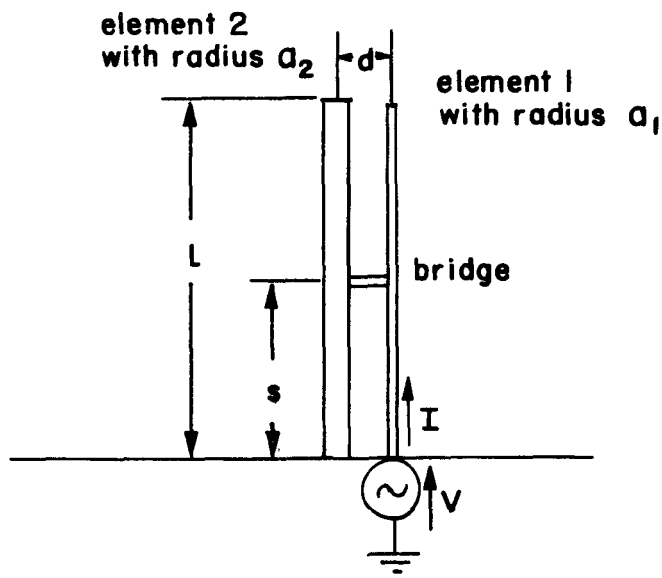

Figure 18--Illustration of the Vertical Folded Monopole with Unequal Elements.

The method of analysis is to resolve the applied voltage into symmetric and antisymmetric parts, and to use superposition to find the total current.

The symmetric and antisymmetric voltages and currents are respectfully V_s, V_a, I_s, and I_a.

The total voltage V is

$$V = V_s + V_a$$

and

$$0 = V_s - V_a \quad ,$$

which implies that $V_s = V/2$ and $V_a = V/2$. Moreover, the total current I is

$$I = I_s + I_a \quad .$$

For the symmetric case, we have the two elements being driven by equal and in-phase sources. We shall assume that the potential of each element in a plane normal to the axis of both elements is equal [4]. Therefore, the bridge can be removed, and the antenna appears as a closely-spaced, in-phase, two-element array, as shown in figure 19.

We have

$$V_{s1} = V_{s2} \quad \text{and} \quad I_{s2} = nI_{s1}$$

Now,

$$V_{s1} = I_{s1} Z_{11} + I_{s2} Z_{12}$$

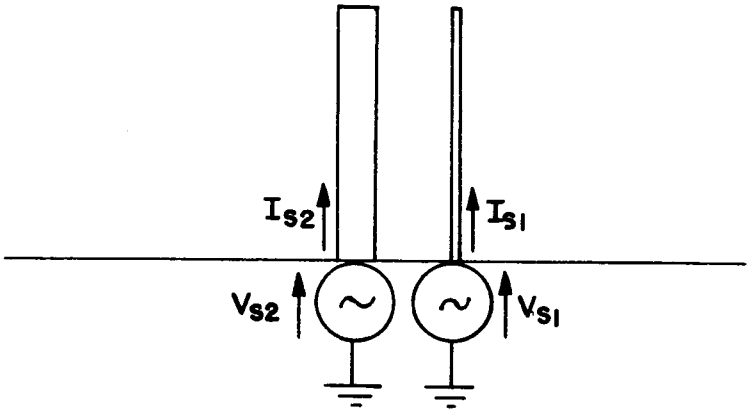

Figure 19--In-Phase Array for the Symmetric Mode.

where Z_{11} is self-impedance of an isolated element and Z_{12} is the mutual impedance between elements one and two. The terminal impedance of element 1 is

$$Z_{s1} = \frac{V_{s1}}{I_{s1}} = Z_{11} + \frac{I_{s2}}{I_{s1}} Z_{12}$$

$$Z_{s1} = Z_{11} + nZ_{12} .$$

Since the distance d is very small, $Z_{12} \approx Z_{11}$, and

$$Z_{s1} = Z_{11}(1 + n) .$$

In the antisymmetric case, we have each element being driven by sources equal in magnitude, but 180° out of phase, and the antenna appears as the short-circuited section of transmission line in figure 20.

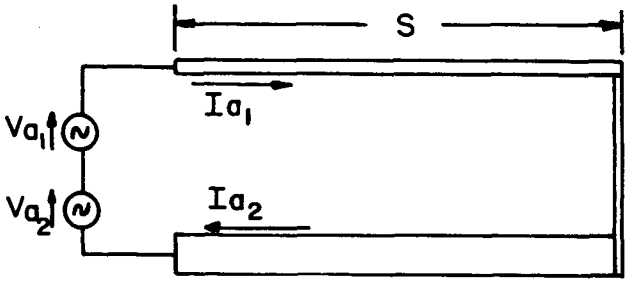

Figure 20--Transmission Line Mode.

The transmission line mode does not radiate appreciably, and the terminal impedance can be found by transmission line methods [5]. Since the antenna does not radiate,

$$I_{a1} = I_{a2} \quad ,$$

and

$$\frac{2V_{a1}}{I_{a1}} = Z_a = jZ_o \tan \frac{2\pi}{\lambda} S, \quad \text{where}$$

Z_o is the characteristic impedance of the transmission line.

The terminal impedance of the antenna is $Z = \frac{V}{I}$

$$I = I_{s1} + I_{a1} = \frac{V_{s1}}{Z_{11}(1+n)} + \frac{2V_{a1}}{Z_a} = \frac{V/2}{Z_{11}(1+n)} + \frac{V}{Z_a}$$

$$I = V \left[\frac{Z_a + 2Z_{11}(1+n)}{2Z_a\, Z_{11}(1+n)} \right] ,$$

and

$$Z = \frac{2Z_a\, Z_{11}(1+n)}{Z_a + 2Z_{11}(1+n)} .$$

From the equation for Z, the equivalent circuit for the antenna is as shown in figure 21, and

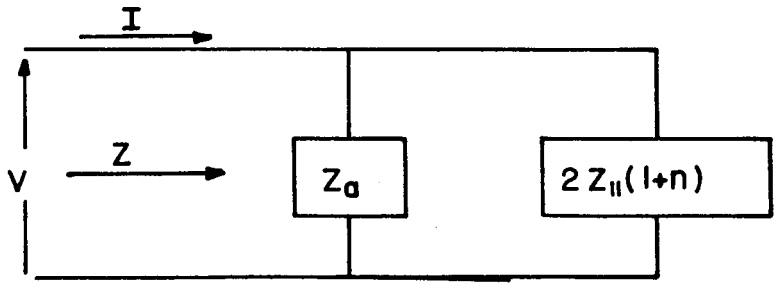

Figure 21--Equivalent Circuit of the Folded Monopole.

The impedance of the antenna can easily be computed if n and Z_o are known.

When calculating the current ratio, if it is assumed that the current is uniformily distributed over a cross-sectional area for both conductors, then the conductors can be replaced by equivalent line sources located at the centers of the elements. The assumption of uniformly distributed current does not take into account the "proximity effect," but for a first order approximation the assumption

should be permittable.

The coordinate system for the antenna is as shown in figure 22.

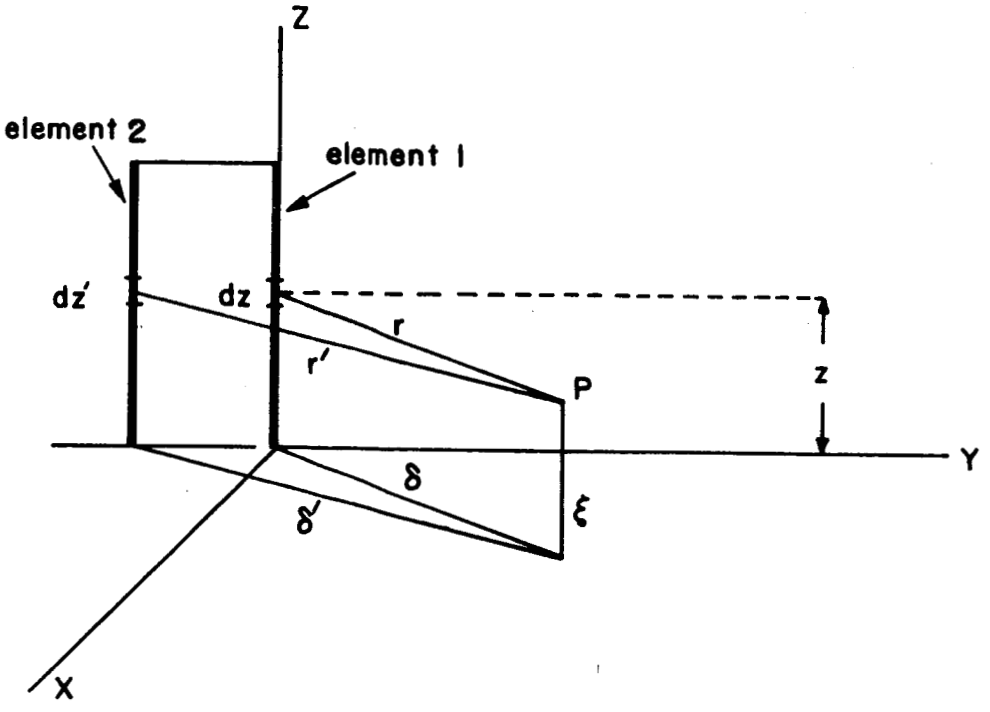

Figure 22--Coordinate System of the Vertical Folded Monopole for the Calculation of n.

We shall first show that the ratio of the charges on the elements is the same as the ratio of the currents. After establishing this we shall use the scalar potential to calculate the ratio of charges.

The equation of continuity is

$$\nabla \cdot \bar{J} + j\omega p = 0 \quad .$$

For the two line sources comprising the antenna, the respective equations of continuity are

$$\frac{\partial I_1(z)}{\partial_z} + j\omega q_1(z) = 0 \qquad (19)$$

$$\frac{\partial I_2(z)}{\partial_z} + j\omega q_2(z) = 0 \quad . \qquad (20)$$

From a previous assumption we have $I_2(z) = n\, I_1(z)$,

$$n \frac{\partial I_1(z)}{\partial z} + j\omega q_2(z) = o \quad . \qquad (21)$$

Multiplying (19) by n and subtracting from (21) we find that

$q_2(z) = n\, q_1(z)$, which is the desired results.

The retarded scalar potential at any point p due to element 1 is

$$\psi = \frac{1}{4\pi\epsilon} \int_{z=0}^{\lambda/4} \frac{1}{r} q_1(z)\, dz \quad .$$

We shall assume that the charge is sinusoidally distributed along the elements, and hence the charge can be written as

$$q_1(z, t) = q_m \cos \frac{2\pi}{\lambda} z \cos(wt - \frac{2\pi}{\lambda} r) \quad [4].$$

Since we are only interested in spatial variations, we can choose a suitable zero time, and thus the charge becomes

$$q_1(z) = qm \cos\left(\frac{2\pi}{\lambda} r\right) \cos\left(\frac{2\pi}{\lambda} z\right),$$

and

$$\psi = k\, q_m \int^{\lambda/4} \frac{1}{r} \cos \frac{2\pi}{\lambda} r \, dz, \text{ where } k = \frac{1}{4\pi\epsilon} .$$

For simplification, we now consider all quantities to be measured in electrical angular degrees. Therefore, $\frac{2\pi}{\lambda} z$ becomes z, and $\frac{2\pi}{\lambda} r$ becomes r.

ψ is now written

$$\psi = k_1 q_m \int_{z=0}^{\pi/2} \frac{1}{r} \cos z \cos r dz, \text{ where } k_1 = \left(\frac{2\pi}{\lambda}\right) k .$$

Now, we make the coordinate transormation

$$z - \zeta = u.$$

Then,

$$\psi = k_1\, q_m \int_{-\zeta}^{\pi/2 - \zeta} \frac{1}{r} \cos (u + \zeta) \cos r \, du.$$

By applying trigonometric identities and re-arranging terms, we obtain

$$\psi = k_1 q_m \frac{\cos \zeta}{2} \left\{ \int_{U_1}^{U_2} \frac{1}{r} \cos(r + u)\, du + \int_{U_1}^{U_2} \frac{1}{r} \cos(r-u)du \right\}$$

$$- \frac{k_1 q_m \sin \zeta}{2} \left\{ \int_{U_1}^{U_2} \frac{1}{r} \cos(r+u)du + \int_{U_1}^{U_2} \frac{1}{r} \sin(r-u)du \right\},$$

where $u_1 = -\zeta$ and $U_2 = \pi/2 - \zeta$.

By transformation of variables, ψ can be put into a form of well tabulated $C_i(x)$ and $S_i(x)$ functions, and, for the first integral, this transformation is as follows:

$$r = u^2 + \partial^2 \quad \text{and} \quad r_1 = u_1^2 + \partial^2, \quad r_2 = u_2^2 + \partial^2 \quad .$$

Let $x = r + u = u^2 + \partial^2 + u$, and

$\int_{u_1}^{u_2} \frac{1}{r} \cos(r + u)du$ becomes

$$\int_{r_1+u_1}^{r_2+u_1} \frac{\cos (x)}{u^2 + \partial^2} \cdot \frac{dx}{\left(\frac{u}{u^2 + \partial^2} + 1 \right)} = \int_{r_1 + u_1}^{r_2 + u_2} \frac{\cos (x)}{x} dx$$

$$= - \int_{-\infty}^{r_1 + u_1} \frac{\cos x}{x}\, dx - \int_{r_2 + u_2}^{\infty} \frac{\cos x}{x}\, dx \quad .$$

Now, in $- \int_{-\infty}^{r_1 + u_1} \frac{\cos x}{x}\, dx$ replace x by -x

giving $- \int_{\infty}^{-(r_1 + u_1)} \frac{\cos x}{x}\, dx = - C_i\left(-(r_1 + u_1)\right)$; but, because

$C_i(x)$ is an even function, $-C_i\left(-(r_1 + u_1)\right) = - C_i(r_1 + u_1)$.

Therefore,

$$\int_{u_1}^{u_2} \frac{1}{r} \cos(r + u)du = -C_i(r_1 + u_1) + C_i(r_2 + u_2) \quad .$$

A similiar procedure for the second, third, and fourth integrals in the equation for Ψ yields:

$$\int_{u_1}^{u_2} \frac{1}{r} \cos(r-u)du = C_i(r_1-u_1) - C_i(r_2-u_2)$$

$$\int_{u_1}^{u_2} \frac{1}{r} \sin(r+u)du = -Si(r_1+u_1) + Si(r_2+u_2)$$

$$\int_{u_1}^{u_2} \frac{1}{r} \sin(r-u)du = Si(r_1-u_1) - Si(r_2-u_2) \quad .$$

Ψ can be put into a more usable form [4] by using the definition:

$C_i(x) = \gamma + \ell n\ X - C_{in}(x)$, where γ = Euler constant. Incorporating this result yields:

$$\psi = k_1 q_m \frac{\cos \zeta}{2} \left[-\ln(r_1+u_1) + C_{in}(r_1+u_1) + \ln(r_2+u_2) - C_{in}(r_2+u_2) + \ln(r_1-u_1) - C_{in}(r_1-u_1) - \ln(r_2-u_2) + C_{in}(r_2-u_2) \right].$$

$$-k_1 q_m \frac{\sin \zeta}{2} \left[-Si(r_1+u_1) + Si(r_2+u_2) - Si(r_1-u_1) + Si(r_2-u_2) \right].$$

Since we are mainly interested in the ratio of charges at the feed point, we can choose the observation point P in the x-y plane. This results in $\zeta=0$. If it is also observed that $\frac{r_2+u_2}{r_1+u_1} = \frac{r_1-u_1}{r_2-u_2}$, then

$$\ln\left\{\frac{(r_2+u_2)\ (r_1-u_1)}{(r_1+u_1)\ (r_2-u_2)}\right\} = 2 \ln \frac{r_2+u_2}{r_1+u_1} \quad , \text{ and}$$

ψ can be written as

$$\psi = \frac{k_1 qm}{2} \left[2 \ln \frac{r_2+u_2}{r_1+u_1} + C_{in}(r_1+u_1) - C_{in}(r_2+u_2) - C_{in}(r_1-u_1) + C_{in}(r_2-u_2) \right].$$

For $\zeta=0$, $u_1=0$ and $u_2 = \pi/2$; moreover, $r_2 = (\pi/2)^2 + \delta^2$ and $r_1 = \delta$. If it is assumed that $\pi/2 >> \delta$ then ψ becomes

$$\psi = \frac{k_1 qm}{2} \left[2 \ln \pi/\delta - C_{in}(\pi) \right].$$

Since the ratio of the charge on element 2 to the charge on

element 1 is n, the potential due to element 2 is

$$\psi' = \frac{k_1 nqm}{2} [2 \ln \pi/\delta' - C_{in}(\pi)], \text{ and}$$

the total potential is $\Phi = \psi + \psi^1$.

Now we can return to the length scale from the angular scale by writing $\frac{2\pi\delta}{\lambda}$ and $\frac{2\pi\delta'}{\lambda}$ in place of δ and δ' respectively. Φ is now written as

$$\Phi = k\, q_m \ln \frac{\lambda^{n+1}}{\delta\delta' n_2 n+1} - k\, qm \left(\frac{n+1}{2}\right) C_{in}(\pi) .$$

The current ratio n can be calculated by setting the potentials at points $X_1 + X_2$ in figure 23 equal:

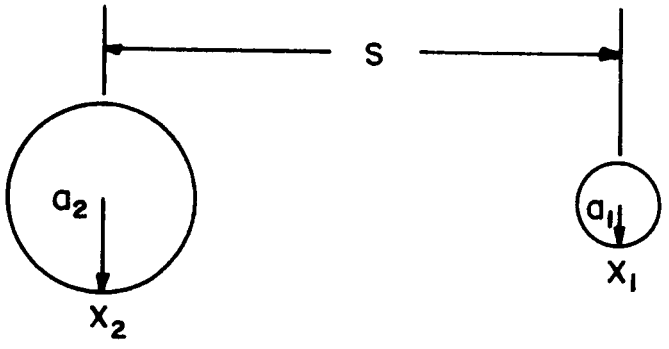

Figure 23--Cross-Section of the Folded Monopole.

$$\Phi(x_2) = k\, q_m \ln \frac{\lambda^{n+1}}{(a_2^2 + s^2)^{1/2} a_2 n_2 n+1} - kqm \left(\frac{n+1}{2}\right) C_{in}(\pi)$$

$$\Phi(x_1) = k\, q_m \ln \frac{\lambda^{n+1}}{a_1 (s^2 + a_1^2)^{n/2} 2n+1} - k\, qm \left(\frac{n+1}{2}\right) C_{in}(\pi) .$$

Setting $\phi(x_2) = \phi(x_1)$ yields:

$$(a_2^2 + s^2)^{1/2}\, a_2^n = a_1(s^2 + a_1^2)^{n/2} .$$

Now, let $b_1 = s^2 + a_1^2$ and $b_2 = a_2^2 + s^2$.

Then we find that

$$n = \frac{\ln a_1/b_2}{\ln a_2/b_1} .$$

Now the characteristic impedance Z_o for a transmission line with a configuration like the bridged-folded monopole must be calculated.

According to King [6], the inductance and capacitance per-unit length for a twin lead transmission line with unequal conductors is

$$L = \frac{u}{2\pi} \left(\cosh^{-1} \psi_1 + \cosh^{-1} \psi_2\right)$$

$$C = 2\pi\epsilon \left(\cosh^{-1} \psi_1 + \cosh^{-1} \psi_2\right)^{-1}$$

with $\psi_1 = \frac{d^2 + a_2^2 - a_1^2}{2 a_1 d}$, $4_2 = \frac{d^2 + a_1^2 - a_2^2}{2a_2 d}$,

where d is the distance between the centers of the two conductors; moreover, a_1 and a_2 are the radii of the conductors.

By knowing L and C, Z_o can be calculated by the formula

$$Z_o = \sqrt{L/C} \quad .$$

V. Experimental Work and Results

The antenna patterns that were recorded for use in this report were made with the antennas positioned on a 20' x 20' ground plane. Although the physical size of the ground plane limited the versatility of the experimental set-up, the data taken at the operating frequency of 138 MHz has more value than if the frequency at which the data was taken had been sealed upward and a smaller ground plane used. We believed that the best results could be obtained by working at the operating frequency of 138 MHz.

The dimensions in wavelengths of a 20' x 20' ground plane at 138 MHz are only 2.28λ x 2.8λ. Since the dimensions are small in terms of wavelengths, the size of the ground plane was investigated experimentally to determine if it was large enough for the antenna to operate properly.

Figures 24.1, 24.2, and 24.3 are antenna patterns that were recorded with a $\lambda/4$ monopole positioned in the center, $\lambda/4$ from the center, and $\lambda/2$ from the center of the ground plane, respectively. Figure 24 illustrates the orientation of the elements.

Figures 24.1, 24.2, and 24.3 reveal that the smallness of the ground plane does have an effect on the patterns. Nevertheless, we felt that since the elements in the direction finding array can be spaced $\lambda/4$ from the center of the ground plane and since the pattern for the element in figure 24.2 is reasonably symmetrical, the size of the ground plane is adequate.

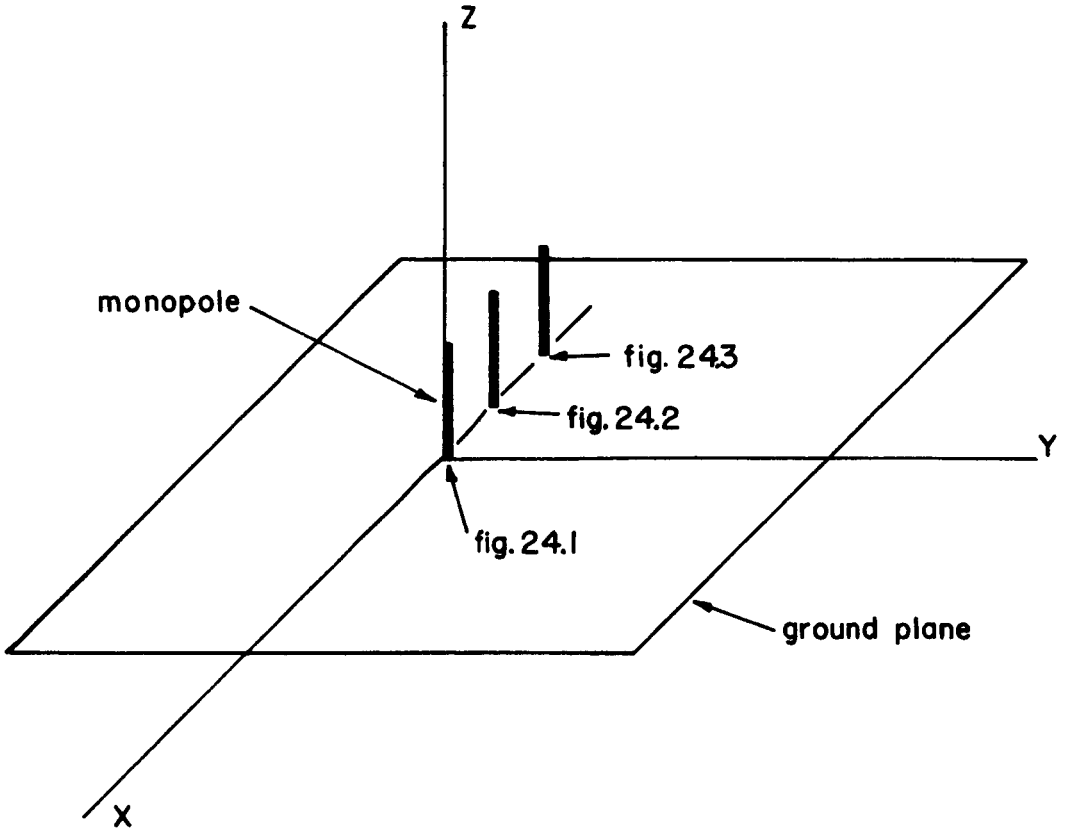

Figure 24--Orientation of the Elements for the Antenna Patterns in Figures 24.1, 24.2, and 24.3.

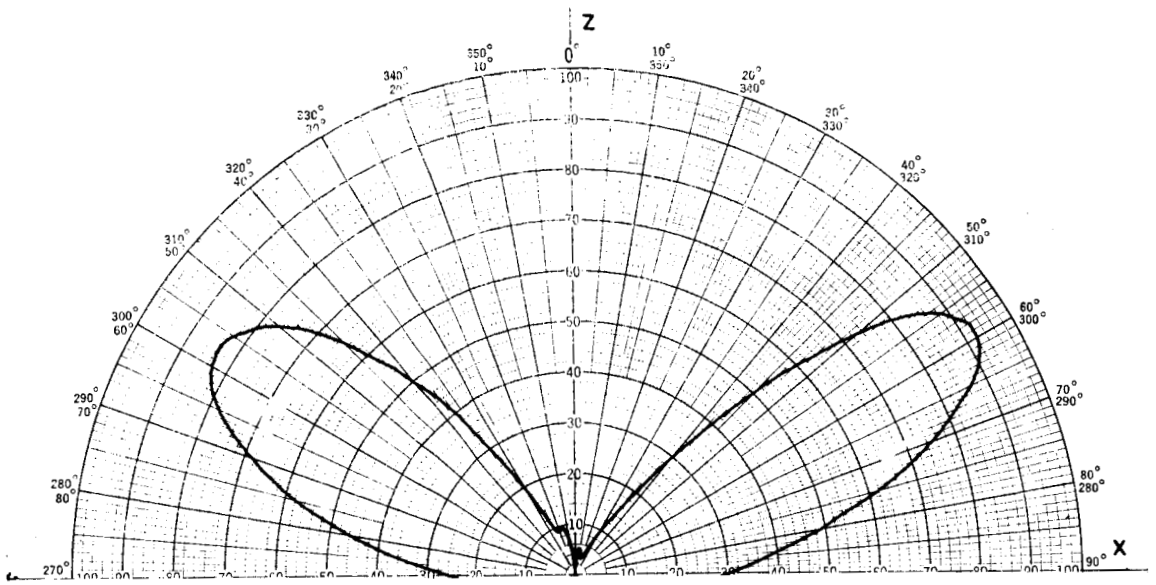

Figure 24.1--Measured radiation pattern of a λ/4 monopole positioned in the center of a 2.8λ X 2.8λ ground plane.

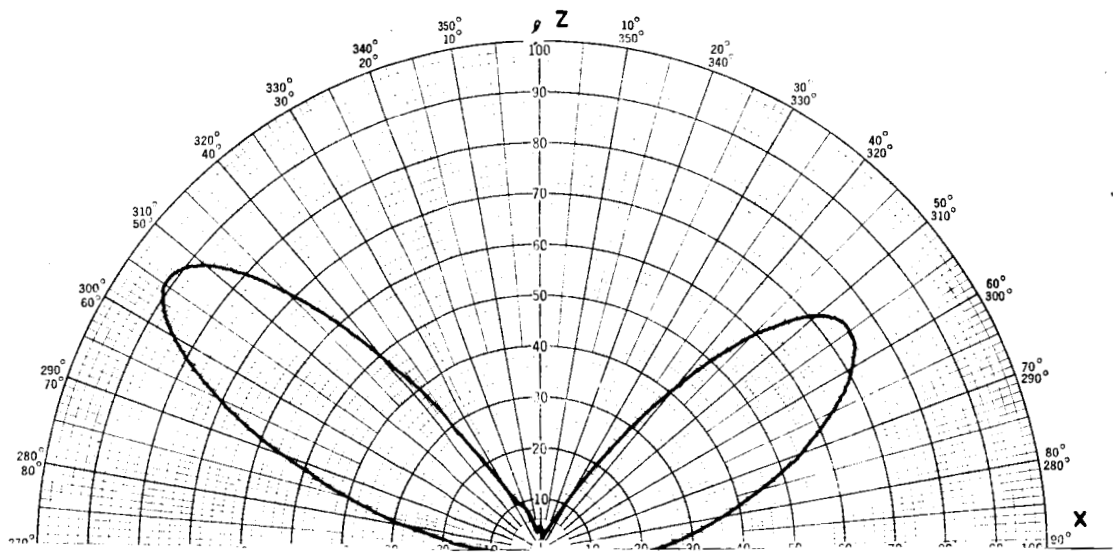

Figure 24.2--Measured radiation pattern of a λ/4 Monopole positioned λ/4 from the center of a 2.8λ X 2.8λ ground plane.

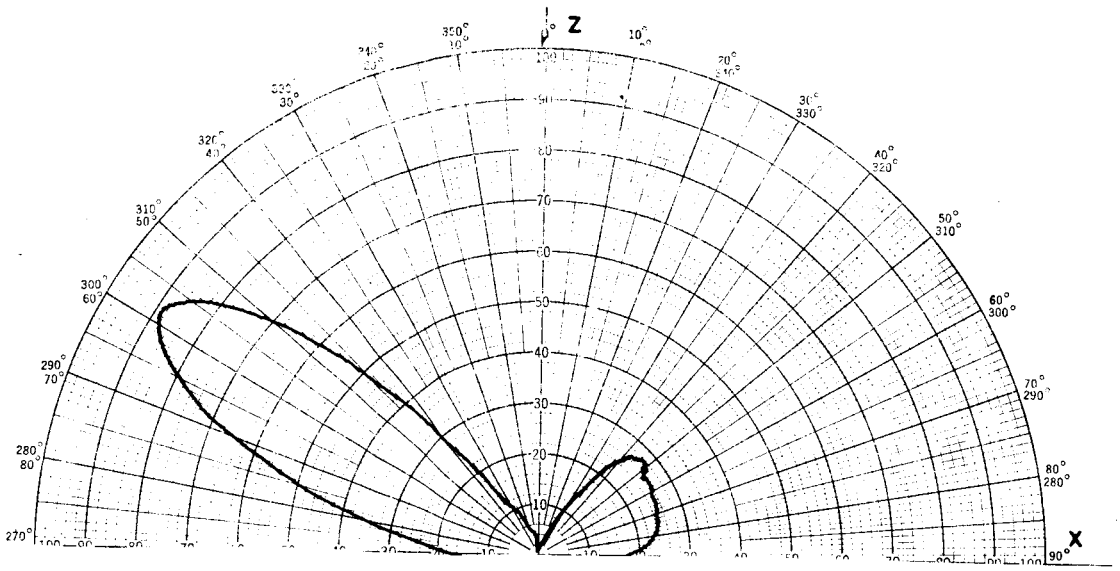

Figure 24.3--Measured radiation pattern of a λ/4 monopole positioned λ/2 from the center of a 2.8λ X 2.8λ ground plane.

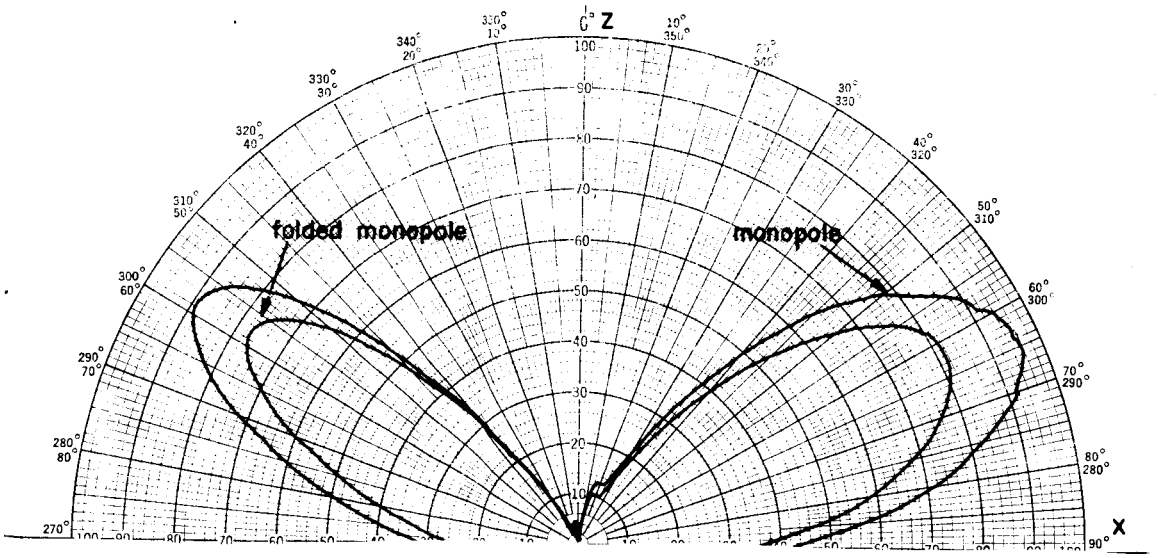

Figure 25--Measured patterns of a single λ/4 monopole and a λ/4 folded monopole.

In Chapter III it was assumed that the horizontal and vertical rings are isolated. As a means of verification, the isolation between the rings was measured and determined to be 31 dbm.

Also in Chapter 3 it was assumed that the $\lambda/4$ folded monopole has the same radiation pattern as a single $\lambda/4$ monopole. Verification of this assumption was accomplished by plotting the pattern of a $\lambda/4$ single monopole, replacing the monopole by a $\lambda/4$ folded monopole, and then plotting the pattern of the folded monopole. The patterns in figure 25 show that the shapes of the two patterns are identical. The difference in amplitude is due to the difference in the element's impedances.

In Chapter IV, Section B, we noted that the height "h" of the dipole above the balum needed to be optimized. An experimental antenna that would enable "h" to be varied while the height of the antenna above the ground plane was held constant was constructed. Patterns of this antenna for different "h's" are shown in figures 26.1, 26.2, 26.3, and 26.4; and from the patterns it is evident that the dipole's pattern is reasonably symmetrical about $\theta=0^{o}$ until h =.1592.

Also, the impedance of the experimental dipole mentioned above was measured for various "h's". From the results of these measurements shown in Table 1, we see that the impedances does not change significantly and that the impedances agree closely with King's [7] theoretical value of 94.1 + j72.4.

h (wavelength)	.00145	.0132	.053	.159
Impedance(ohm)	95+j64	97+j65	100+j70	110+j71

Table 1--Impedance of a $\lambda/4$ Dipole Above a Ground Plane.

We decided that the optimum height "h" is .00145 λ, which is .125 of an inch at 138 MHz. This height was chosen because the pattern at this height is as symmetrical as the patterns for the other heights and because the smaller the "h" is the closer the length of the balun approaches $\lambda/4$, which is the height chosen for the vertical folded monopoles.

In the section on the analysis of the impedance of a bridged folded monopole, the impedance was found to be $Z = \frac{2Z_a Z_{11}(1+n)}{Z_a + 2Z_{11}(1+n)}$. The vertical elements used in the direction finding array had the following dimensions: a_1=1/16", a_2=1/2", and b = 5/8". Using these dimensions, n was calculated as 2.59. Z_o was determined to be 170 ohms. Z_{11}, taken from King's [8] second order approximations, was found to be (42 + j22).

Using these parameters, Z was calculated for different heights, "s", of the bridge above the ground plane or antenna terminal. The results are shown in Table 2.

The impedance of an identical antenna was calculated by King [7] for the case when s = $\lambda/4$; he found the impedance to be Z = 224.5 + j169.7. This value agrees with the value of Z in Table 2 when S = 21 inches; and for all practical considerations, 21 inches in wavelengths at 138 MHz is $\lambda/4$.

S(inch)	Z(ohm)
6	12.2 + j63.4
7	16.6 + j73.4
8	21.7 + j83.3
10	34.6 + j103.0
12	52.0 + j122.6
14	75.5 + j169.5
16	107.6 + j158.5
18	151.7 + j169.5
21	244.5 + j153.7

Table 2--Calculated Impedance of a Bridged Folded Monopole of Unequal Elements.

Admittance measurements for different values of "s" were made on a single element with the dimensions given above. These admittances along with their equivalent impedances are shown in Table 3. These measurements were made with the antenna positioned on a horizontal 20' x 20' ground plane.

S(inch)	Y(10^{-3}mho)	Z(ohm)
6	2.0 -j7.5	33.2 + j124.5
7	2.0 -j6.0	50 + j150
8	2.0 -j4.9	71.5 + 175
10	2.0 -j2.7	177 + j239
12	2.0 -j1.4	336 + j235
14	2.0 -j0.02	500 + j5
16	2.0 -j0.6	460 + j138
18	2.0 -j1.6	305 + j244
21	2.0 -j2.6	186 + j242

Table 3--Measured Admittance and Impedance of a Bridged Folded Monopole of Unequal Elements.

From the admittance measurements we see that the imagninary part of the admittance did change with s, but the real part did not change. This verifies that the method of analyzing the antenna as the superposition of a radiation and transmission line mode is correct. This can be recognized by considering the two impedances in the

equivalent circuit of figure 21 to be admittances. The admittance of the radiation mode, $\frac{1}{2Z_{11}(1+n)}$, is solely determined by the dimensions of the antenna; but the transmission line mode admittance, $\frac{1}{Z_a} = \frac{1}{jZ_o \tan\frac{2\pi}{\lambda}s}$, is a function of s and purely imagniary. Since admittances add when they are connected in parallel, the real part of the total antenna admittance should not change with s.

Tables 2 and 3 indicate that there are differences between the calculated and the measured impedance of the antenna. The difference is contributed to the fact that in the analysis of the antenna the ground plane was considered to be infinite in size, but the size of the ground plane on which the measurements were made was relatively small as is illustrated in figures 24.1, 24.2, and 24.3.

For the direction finding system to operate optimumly, each element should be matched to the transmission line it feeds for the following reasons: (1) so that all the power available will be transferred to the transmission lines, and (2) so that there will not be a mismatch in the feed system caused by a multicoupler not being terminated in a matched impedance.

Single-stub tuners were the devices used for matching the elements; and since the vertical and horizontal rings are isolated, each ring was independently matched.

For the vertical ring, placement of the bridge on the folded monopoles made it possible to select an impedance that could be easily matched.

The procedure for matching each ring was to terminate

each element with adjustable single-stub tuner, and then to terminate three of the tuners with 50 ohm terminations (which is the input impedance to one of the multicouplers when matched output conditions are assumed). The fourth tuner was then adjusted until the antenna element was matched. After that tuner had been terminated in 50 ohms, one of the other tuners was adjusted until that element was matched. This procedure was continued until all the elements had been matched.

In Chapter IV, an experimental method for normalizing the sequence voltages was described. For this method, the relative values of the $f_i(\theta,\phi)$ have to be known at some pointing (a specific θ and ϕ). Because of the smallness in wavelengths of the ground plane, more accurate results can be obtained by actually measuring the $f_i(\theta,\phi)$ than by using theoretical values. The $f_i(\theta,\phi)$ for the vertical ring are shown in figures 27.1, 27.2, 27.3, and 27.4. Patterns of the sequence voltages for the vertical ring are shown in figures 28.1, 28.2, 28.3, and 28.4.

It must be pointed out that the patterns are plotted in units of power, and whenever it is necessary to know the relative amplitude of the voltage of one pattern to the amplitude of the voltage of another pattern, the square root of the relative power may be used. Also, refer to figure 1 for the orientation of the antennas.

Except for the pointing, the procedure used for normalization of the sequence voltages of the vertical ring is identical with the procedure described in Chapter IV. The pointing actually used is $\theta = 60^{\circ}$, $\phi = 0$. After substituting the relative magnitudes of the

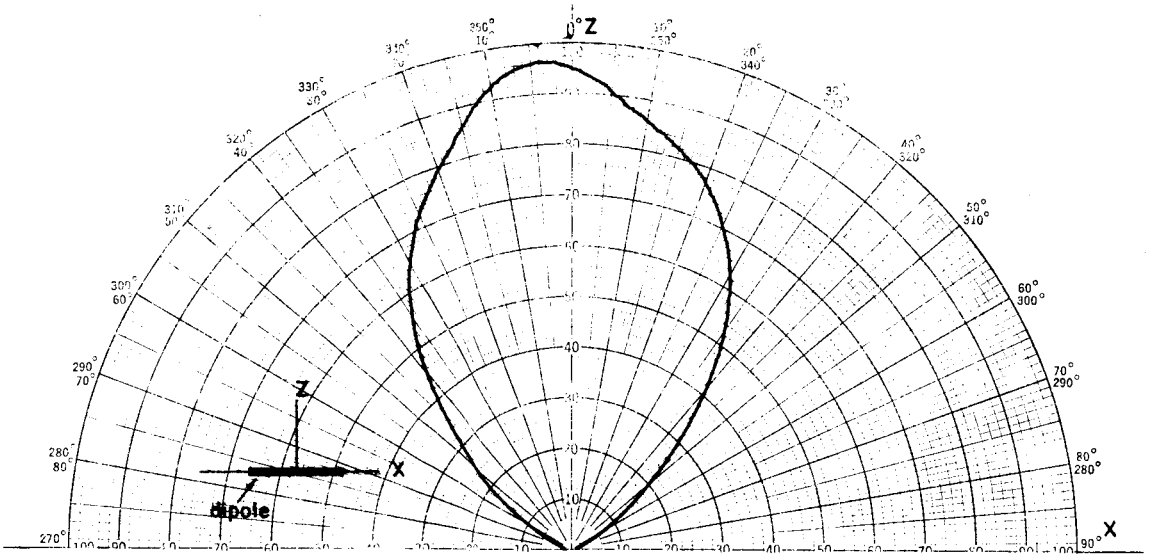

Figure 26.1--Measured pattern of a horizontal dipole with h = .001452

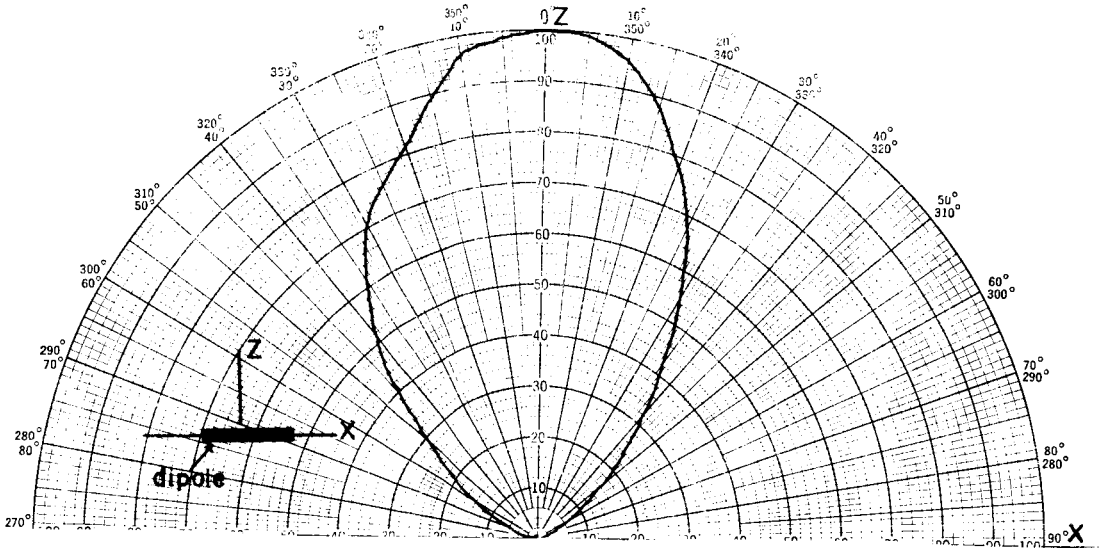

Figure 26.2--Measured pattern of a horizontal dipole with h = .0132 λ

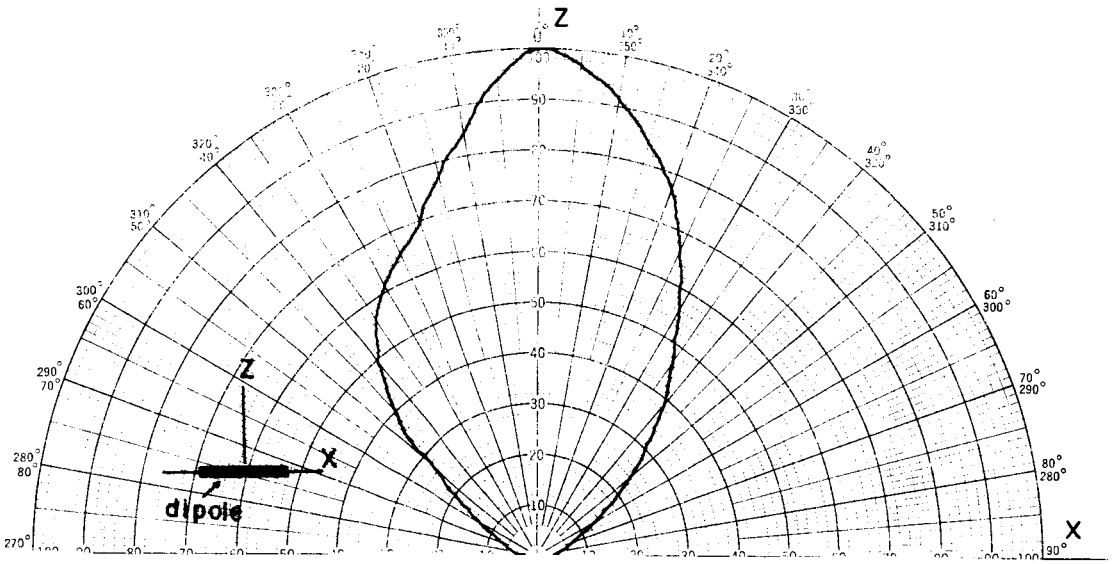

Figure 26.3--Measured pattern of a horizontal dipole with h = .053λ

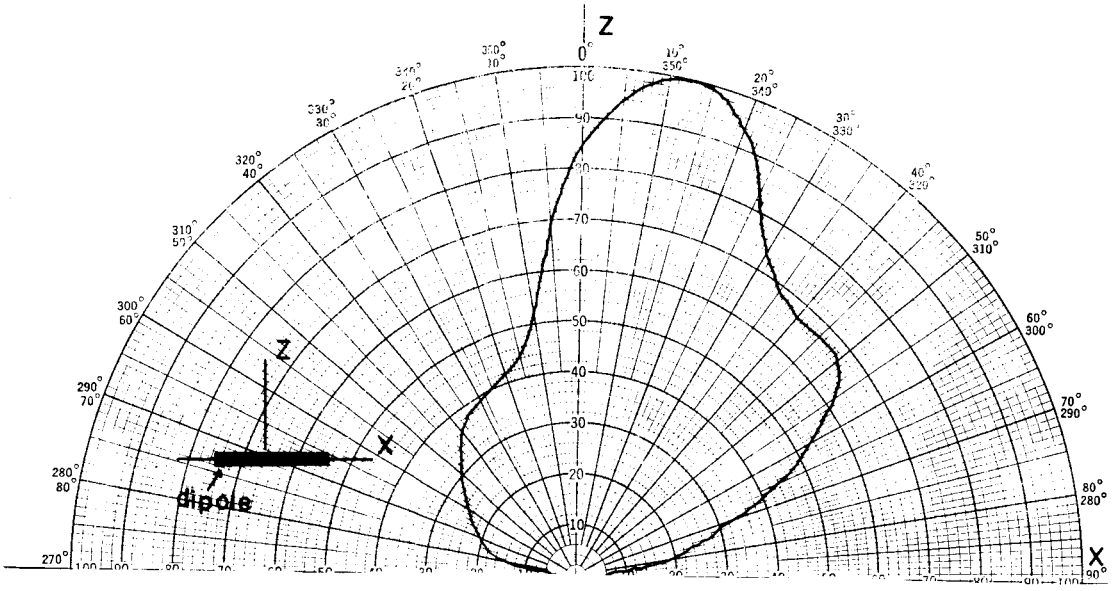

Figure 26.4--Measured pattern of a horizontal dipole with h = .159 λ

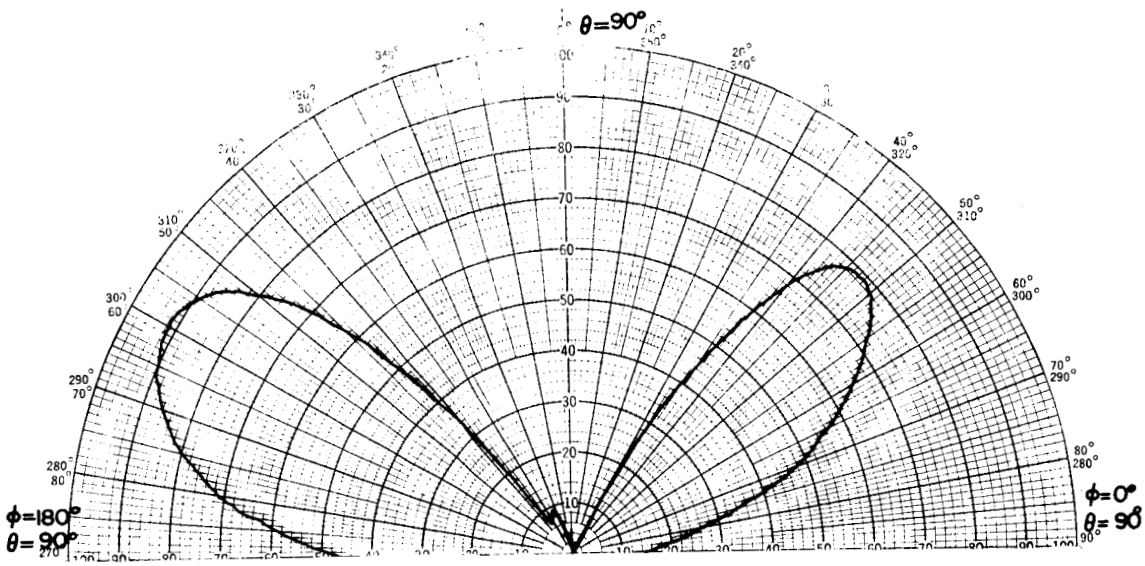

Figure 27.1--Measured radiation pattern of element #1 of the vertical ring. 8 db attenuation.

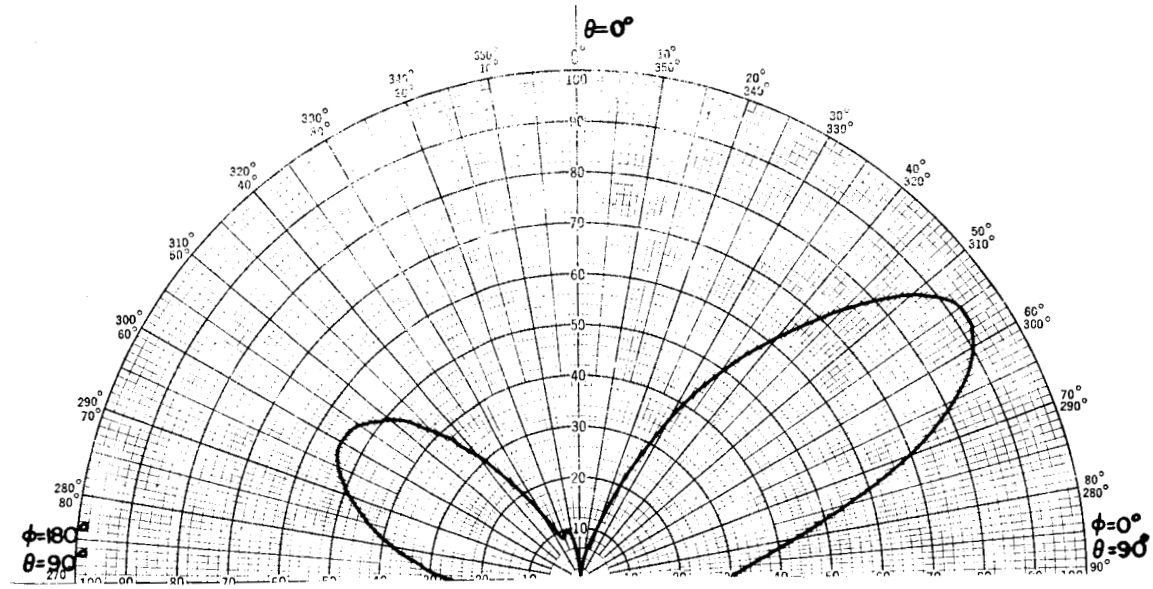

Figure 27.2--Measured radiation pattern of element #2 of the vertical ring. 9.5 db attenuation.

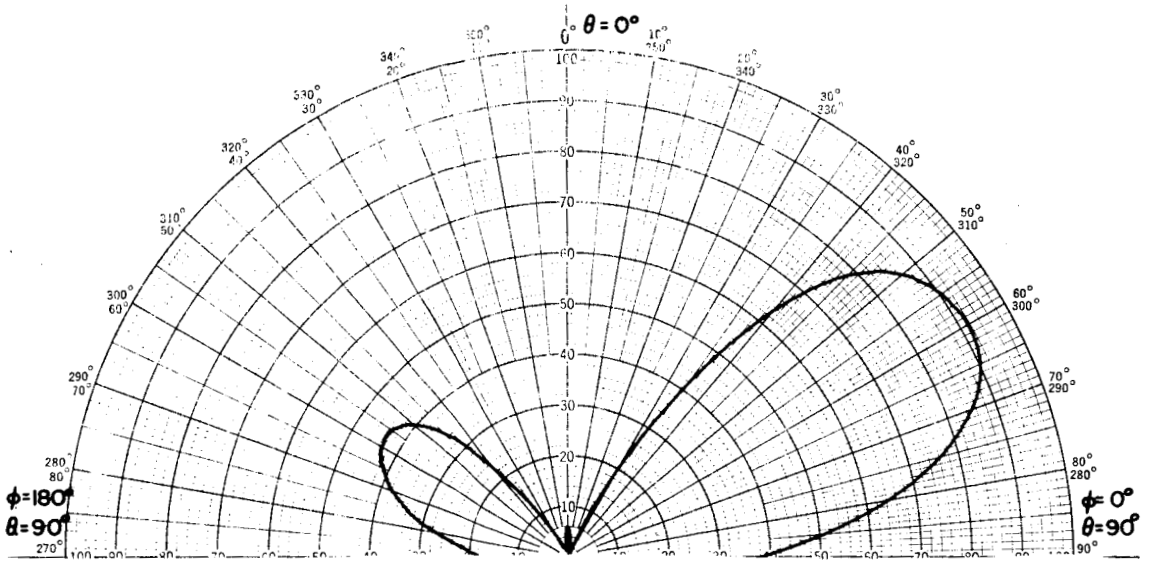

Figure 27.3--Measured radiation pattern of element #3 of the vertical ring. 11db attenuation.

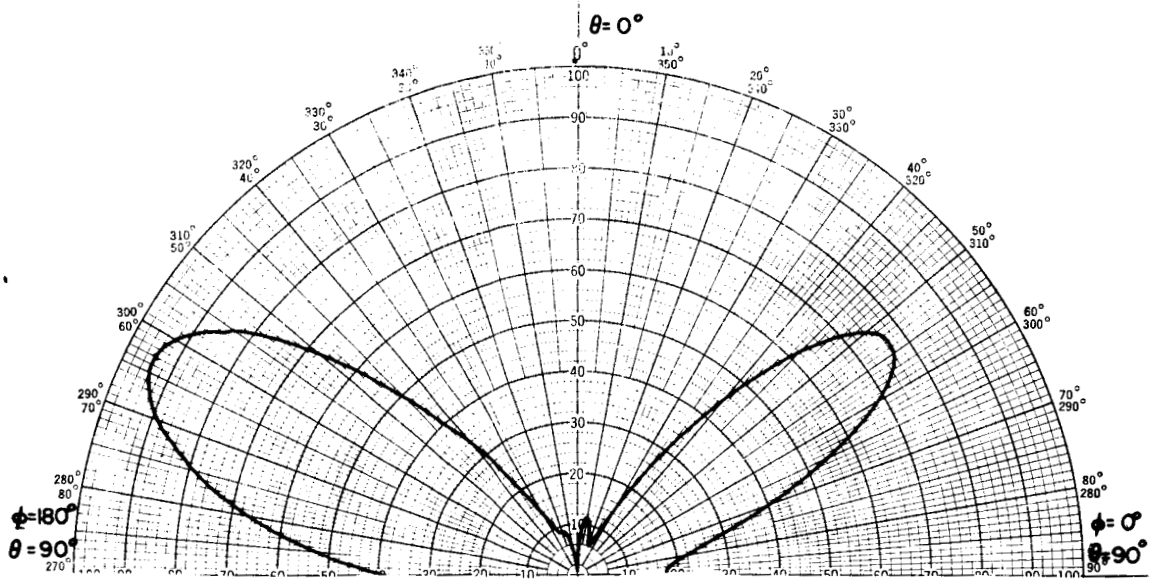

Figure 27.4--Measured radiation pattern of element #4 of the vertical ring. 10db attenuation.

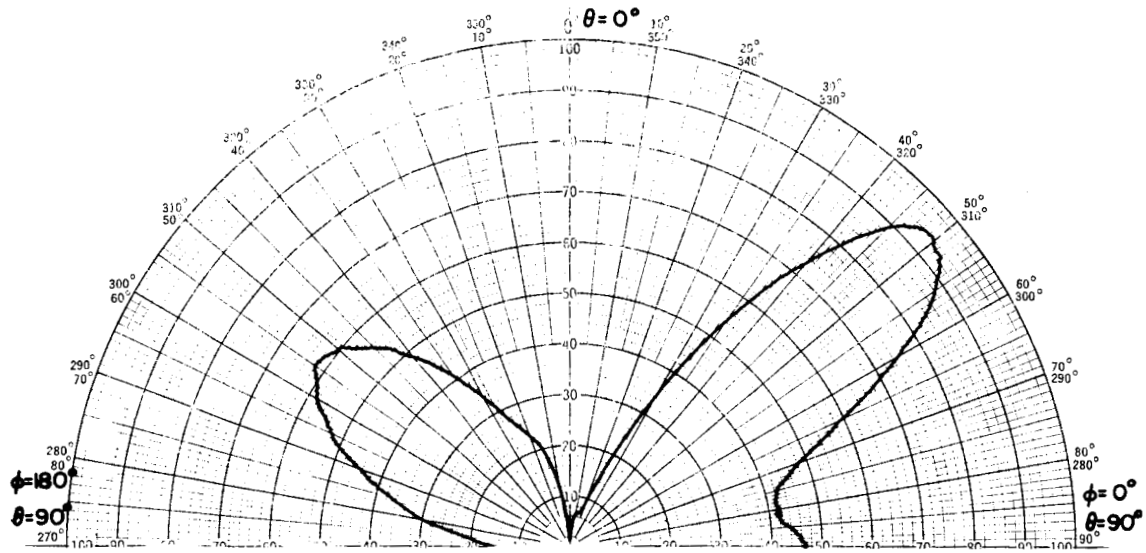

Figure 28.1--Measured pattern of $V_v^{(0)}$ as a function of θ and ϕ. 14 db attenuation.

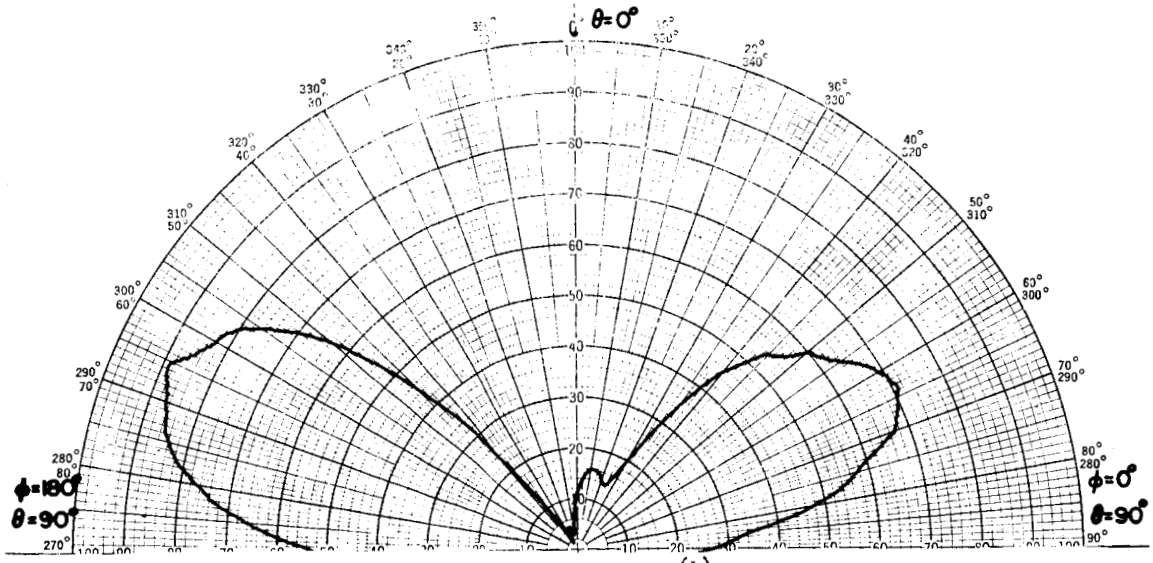

Figure 28.2--Measured pattern of $V_v^{(1)}$ as a function of θ and ϕ. 12 db attenuation.

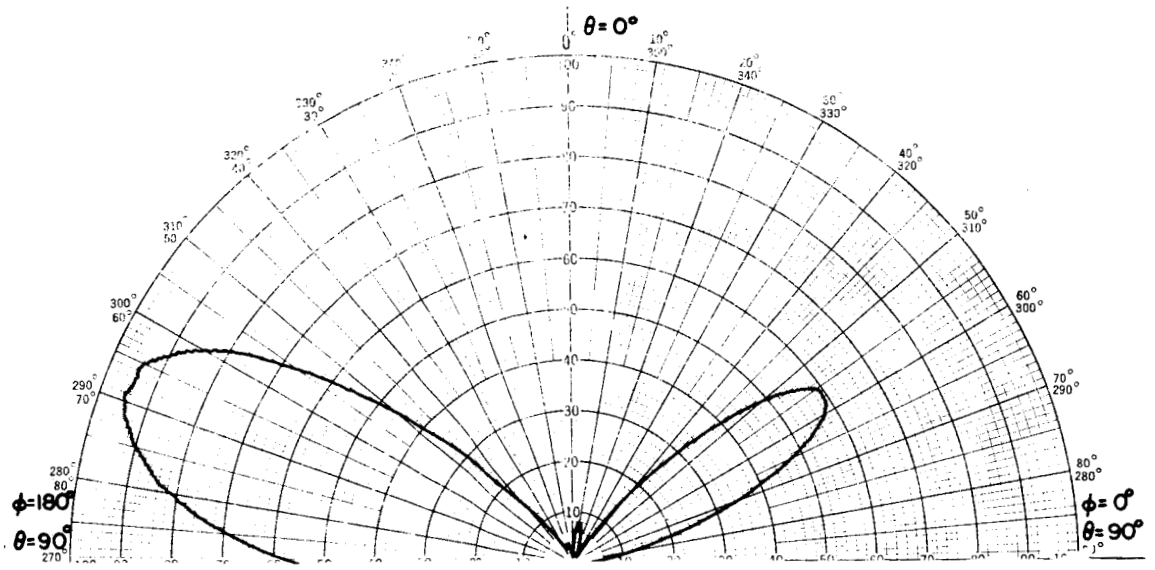

Figure 28.3--Measured pattern of $V_v^{(2)}$ as a function of Θ and Φ. 14 db attenuation.

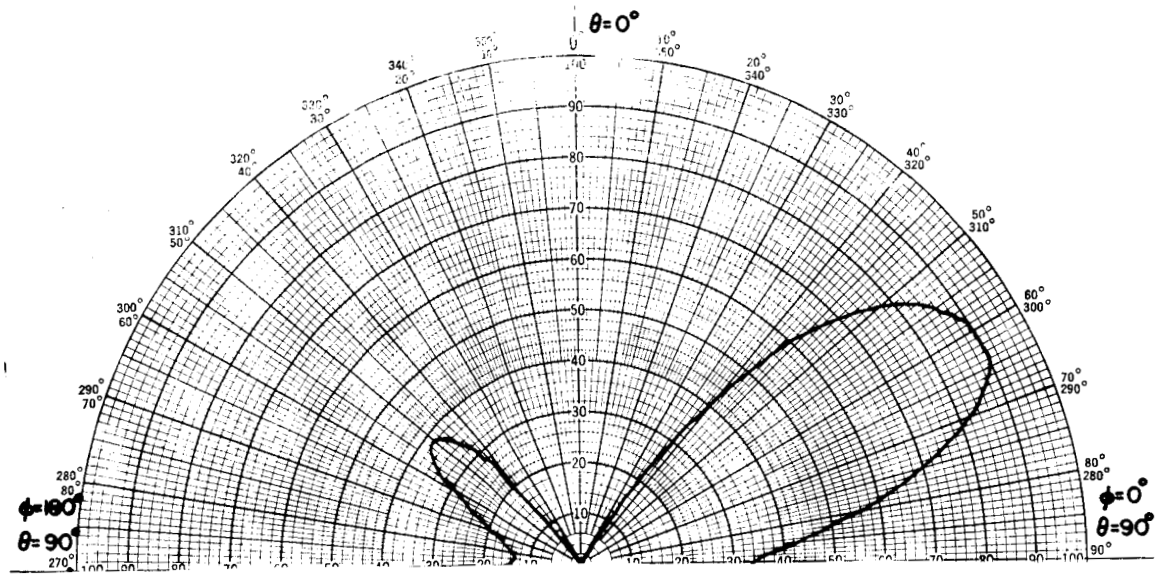

Figure 28.4--Measured pattern of $V_v^{(3)}$ as a function of Θ and Φ. 12.5 db attenuation.

$f_i(\Theta,\phi)$ into equations for the sequence voltages, and after simplification, we find

$$V^{(0)} = (1.98)\ \frac{VR}{|Z^{(0)}|}\ e^{-j\phi_0}\ e^{-j11.4^\circ}$$

$$V^{(1)} = (1.62)\ \frac{VR}{|Z^{(1)}|}\ e^{-j\phi_1}\ e^{j90^\circ}$$

$$V^{(2)} = (1.33)\ \frac{VR}{|Z^{(3)}|}\ e^{-j\phi_2}\ e^{j162.8^\circ}$$

$$V^{(3)} = (1.5)\ \frac{VR}{|Z^{(3)}|}\ e^{-j\phi_3}\ e^{j90^\circ}\ .$$

Now, by substituting the relative magnitudes of the sequence voltages, taken from the patterns, into the above equations, we find the relative magnitudes of the sequence impedances to be

$$|Z^{(0)}| = (1.98)VR$$

$$|Z^{(1)}| = (2.14)VR$$

$$|Z^{(2)}| = (1.53)VR$$

$$|Z^{(3)}| = (1.64)VR\ .$$

It is the relative magnitudes of the sequence impedances that must be compensated for.

From figure 2, we notice that before the sequence voltages are combined into V_1 and V_m, the zero sequence voltage is divided three

ways while the other sequence voltages are divided only two ways. This requires all the sequence voltages except $V^{(0)}$ to be decreased by $(2/3)^{1/2}$.

The attenuation needed for normalization of the magnitudes of the sequence voltages is

$V^{(0)}$ 0 db

$V^{(1)}$ 1.14 db

$V^{(2)}$ 4.2 db

$V^{(3)}$ 3.4 db .

The phase angles of the sequence voltages were measured with respect to a suitable reference in order to normalize the phase angles of the sequence voltages. These phase measurements are tabulated in table 4.

	$V^{(0)}$	$V^{(1)}$	$V^{(2)}$	$V^{(3)}$
Phase Lag	180^{o}	153^{o}	48.4^{o}	120.5^{o}

Table 4--Phase Lag of the Sequence Voltages of the Vertical Ring at $\theta = 60^{o}$, $\phi=0$ with Respect to Reference Phase.

By the method described in Chapter IV for the phase normalization, we found that the sequence voltages needed the following phases added

$V^{(0)}$ - - - - - 75^{o}

$V^{(1)}$ - - - - - 0^{o}

$V^{(2)}$ - - - - - 32^{o}

$V^{(3)}$ - - - - - 33^{o}.

The steps taken in normalizing the sequence voltages of the horizontal ring are the same as the ones used for the vertical ring. The pointing that was used is $\theta = 30^{0}$, $\phi = 45^{o}$. The patterns needed for normalization of the horizontal ring are shown in figures 29.1 through 30.4. The phase measurements for the horizontal ring are in table 5.

	$V^{(0)}$	$V^{(1)}$	$V^{(2)}$	$V^{(3)}$
Phase Lag	121.9^{o}	174.1^{o}	61.6^{o}	123^{o}

Table 5--Phase Lag of the Sequence Voltages of the Horizontal Ring at $\theta=30^{o}$, $\phi=45^{o}$ with respect to Reference Phase.

The attenuation that should be inserted in each sequence voltage of the horizontal ring is

$V^{(0)}$ - - - - - 0 db

$V^{(1)}$ - - - - - 8.2 db

$V^{(2)}$ - - - - - 16.5 db

$V^{(3)}$ - - - - - 5.9 db .

The amount of phase that should be added to each sequence voltage of the horizontal ring is

$v^{(0)}$ - - - - - 176.8^{o}

$v^{(1)}$ - - - - - 0^{o}

$v^{(2)}$ - - - - - 197.9^{o}

$v^{(3)}$ - - - - - 123.9^{o}.

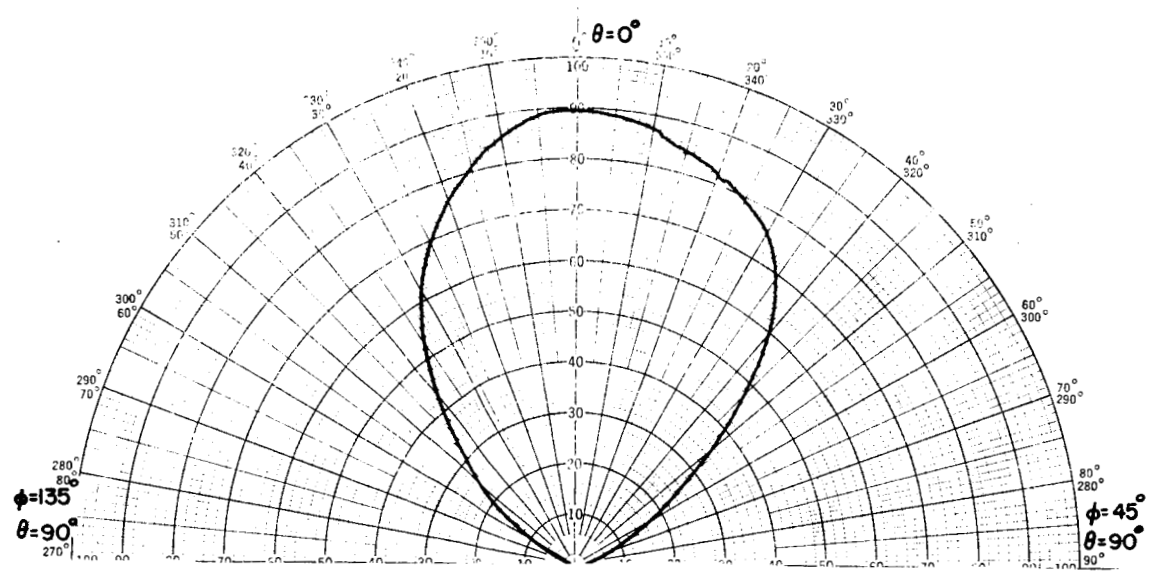

Figure 29.1--Measured radiation pattern of element #1 of the horizontal ring. 13.5 db attenuation.

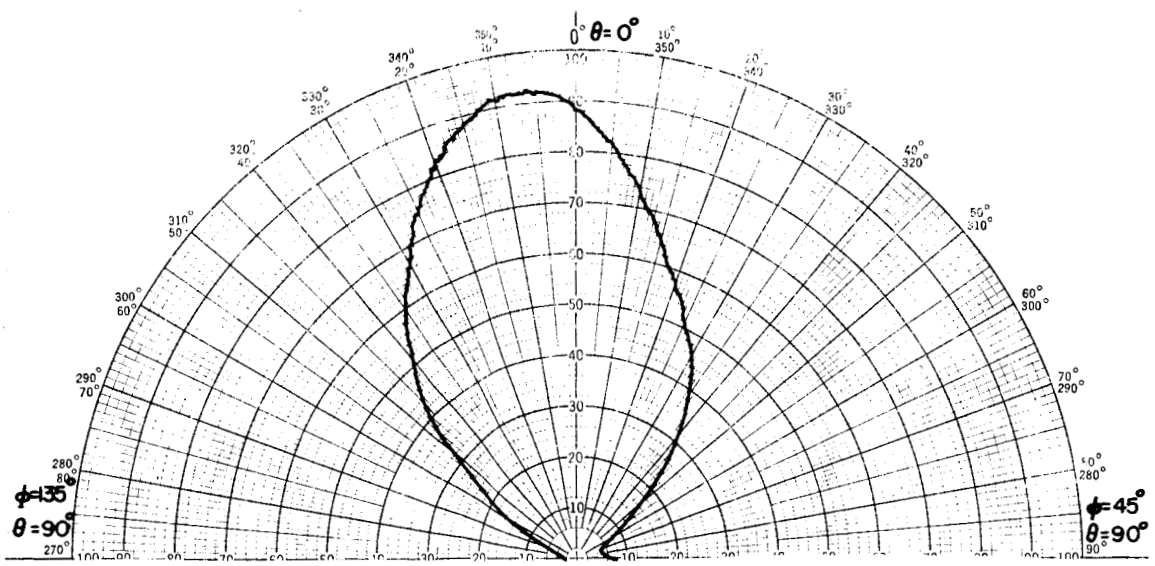

Figure 29.2--Measured radiation pattern of element #2 of the horizontal ring. 10db attenuation.

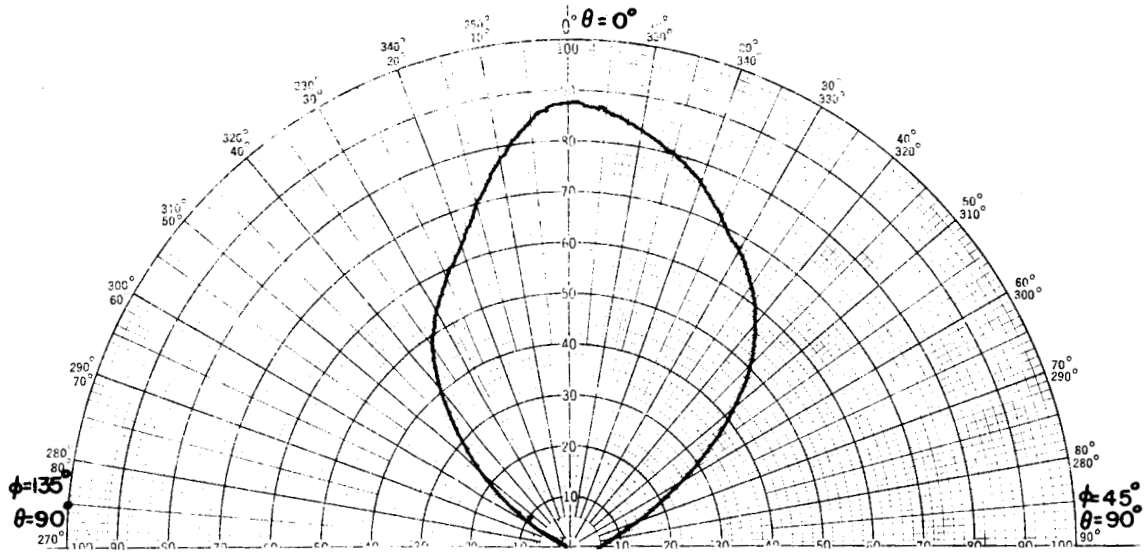

Figure 29.3--Measured radiation pattern of element #3 of the horizontal ring. 11.5 db attenuation.

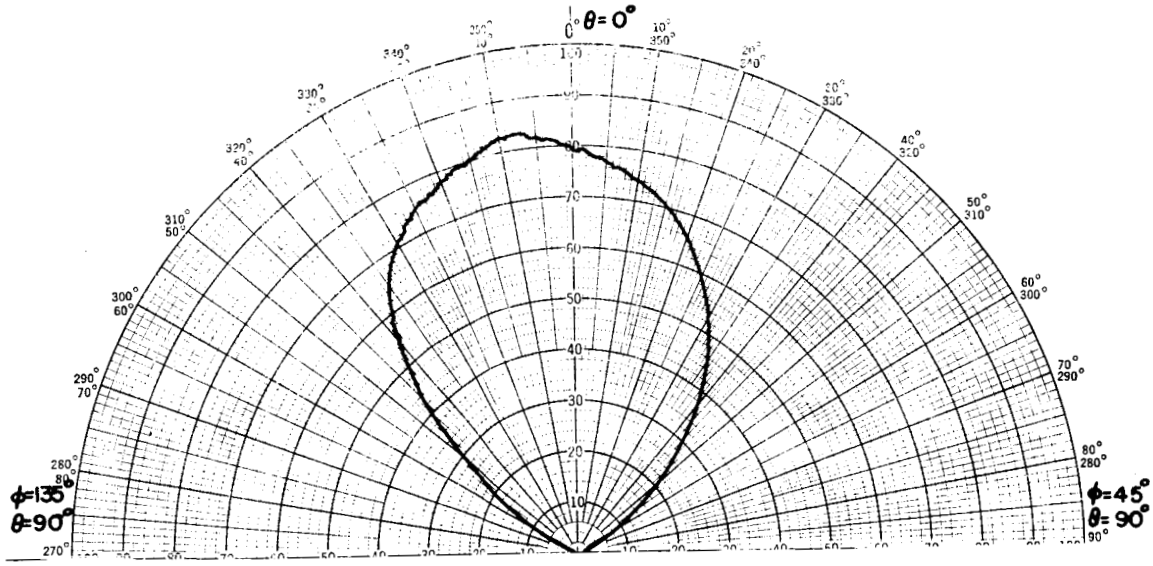

Figure 29.4--Measured radiation pattern of element #4 of the horizontal ring. 13 db attenuation.

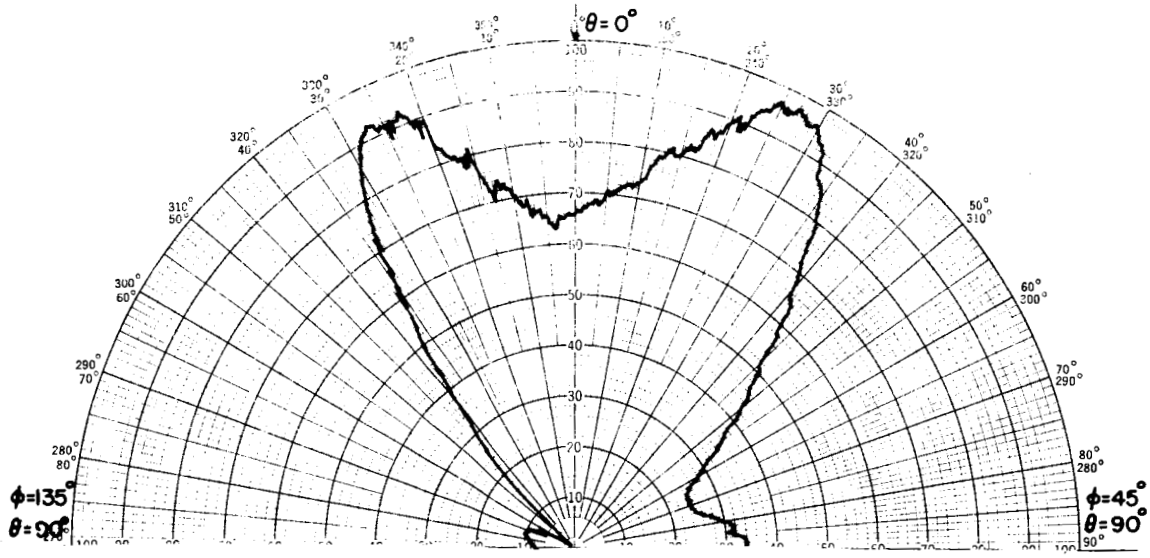

(0)
Figure 30.1--Measured pattern of V_H as a function of θ and φ. 19.5 attenuation.

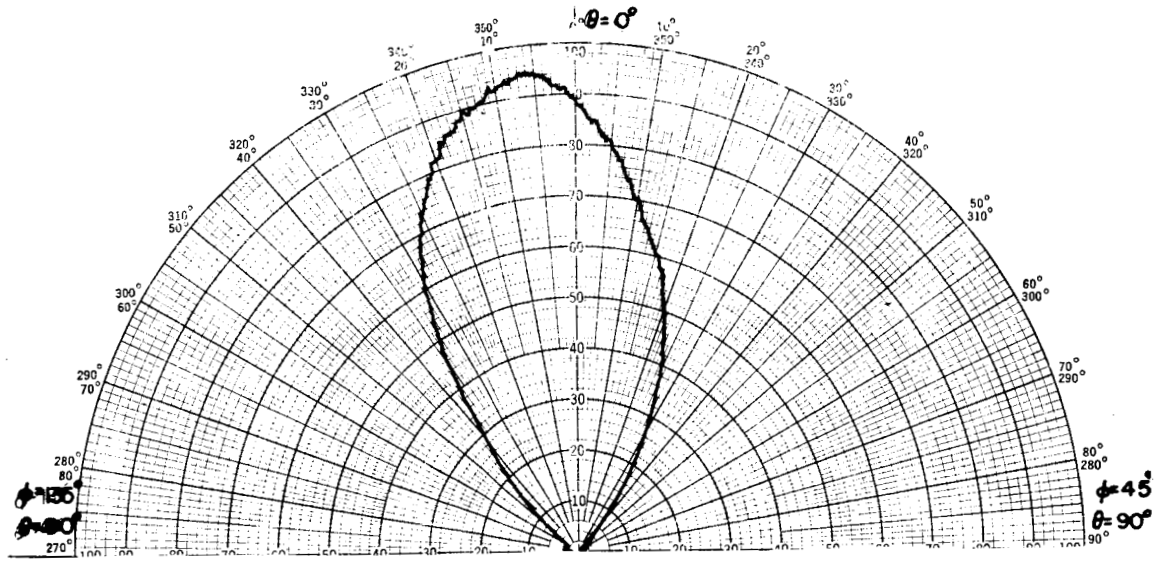

Figure 30.2--Measured pattern of $V_H^{(1)}$ as a function of θ and φ. 22.5 db attenuation.

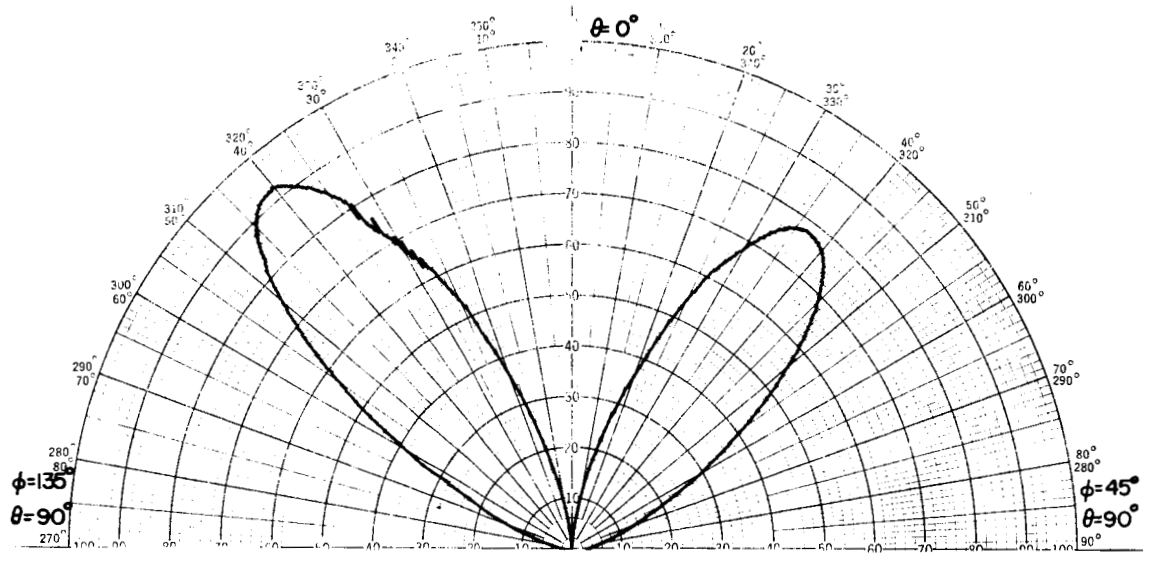

Figure 30.3--Measured pattern of $V_H^{(2)}$ as a function of θ and φ. 21 db attenuation.

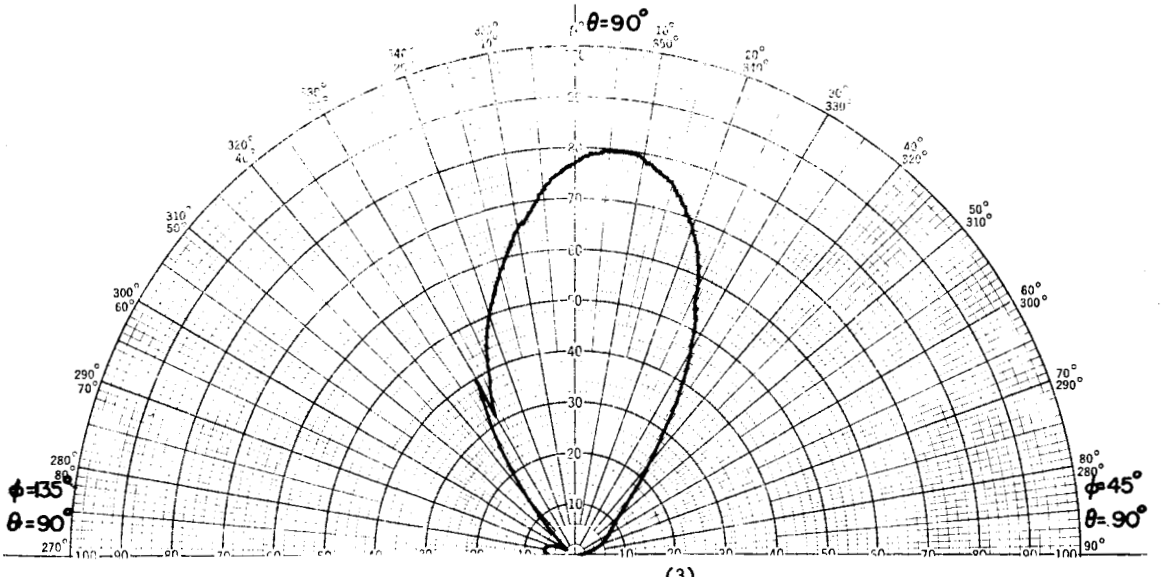

Figure 30.4--Measured pattern of $V_H^{(3)}$ as a function of θ and φ. 225 db attenuation.

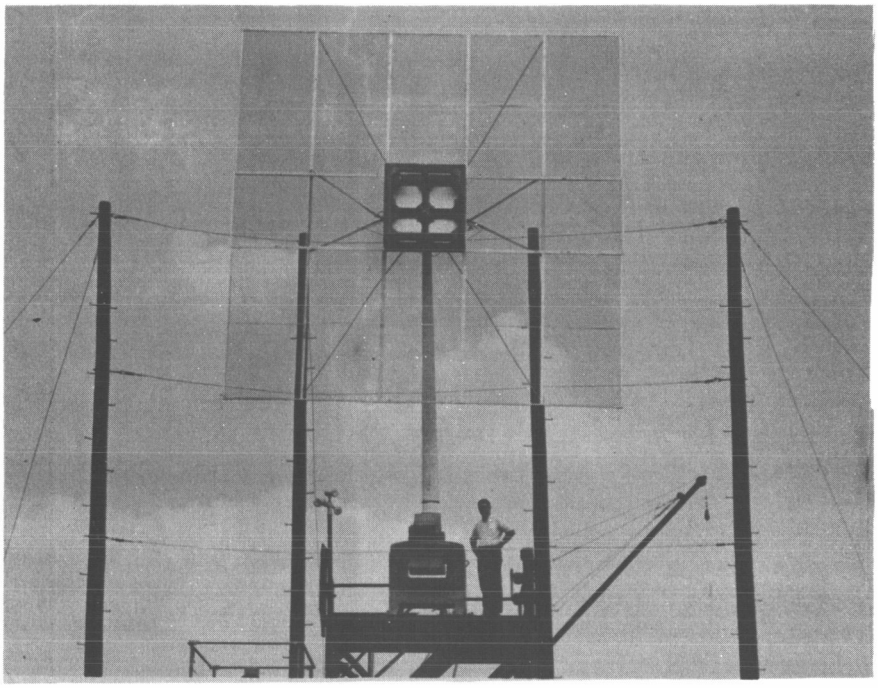

Figure 31--Photograph of Direction Finding Antenna and Ground Plane Mounted on Antenna Positioner.

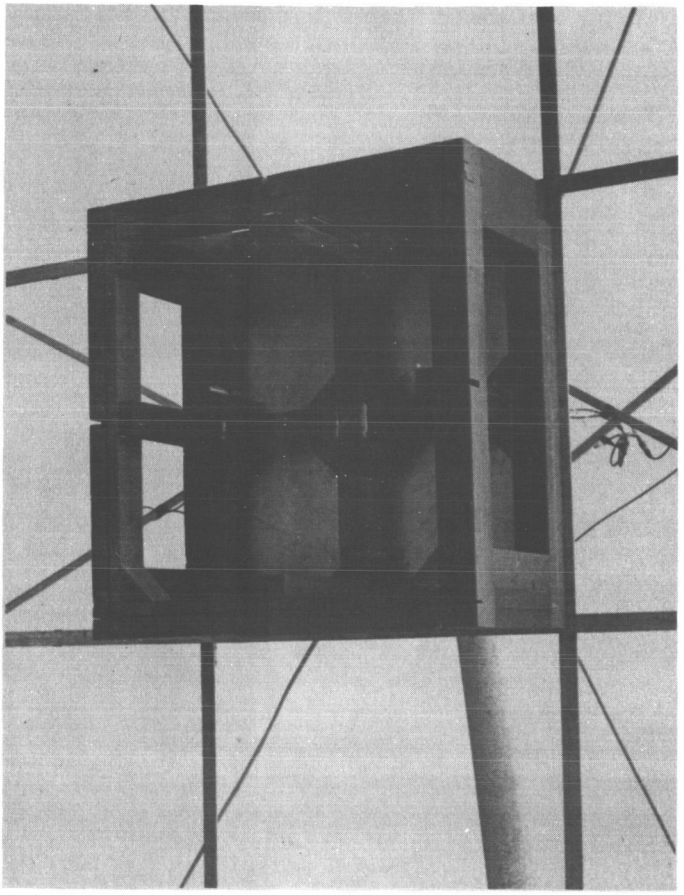

Figure 32--Photograph of direction finding antenna

VI. CONCLUSIONS

A direction finding system that derives the direction cosines of the direction of arrival of a radio frequency signal has been presented. Since the direction finding antenna must be omnidirectional and must respond to a signal of any given polarization, the antenna should consist of a vertical and a horizontal ring. Although the use of two rings necessitates the use of two feed systems, it was decided that this is the best method of fulfilling the specified directional characteristics and polarization requirements. In light of the low frequency of operation, it is believed that the elements used in the direction finding array are optimum.

Although the multicouplers employed in the feed system function properly in generating the sequence voltages, they have the undesirable characteristic of power dissipation in the isolation resistors. These multicouplers are the best available at the present time, and future work on a similar feed system should be directed towards finding a multicoupler that does not dissipate any power.

The method of normalizing the sequence voltages originated with this study should allow accurate direction information to be obtained.

REFERENCES

[1] H.P. Neff, Jr., "A Radio Frequency Direction Finding System Employing Direction Cosines", Dissertation, Department of Electrical Engineering, Auburn University, 1967.

[2] John D. Kraus, Antennas (New York: McGraw-Hill Book Company, 1950) p. 142.

[3] John F. Randolph, Calculus and Analytic Geometry (Belmont, California: Wadsworth Publishing Company, 1961) p. 310

[4] Rudolph Guertler, "Impedance Transformation in Folded Dipoles", Pro. of the I.R.E., p. 1044, September, 1950.

[5] Ronald W. P. King, Transmission-line Theory (New York: Dover Publications, Inc., 1965) p. 28.

[6] Ronald W. P. King, The Theory of Linear Antennas (Cambridge, Massachusetts: Harvard University Press, 1956) p. 339.

[7] Ronald W. P. King, The Theory of Linear Antennas (Cambridge, Massachusetts: Harvard University Press, 1956) p. 280.

[8] Ibid., p. 361.